Our replies to referees' comments are inserted in red below. The marked-up revised manuscript is appended at the end.

Reviewer 1

The authors construct a data record of sea ice extents and ice type coverage (multiyear, second year, and first-year ice) from satellite scatterometers (ERS, QuikSCAT, ASCAT) that show the loss of sea ice and old ice over the last 25 years. Relatively good agreements between thicknesses classes from CryoSat-2 and the ice types suggest that the ice types could be reliable proxies of sea ice thickness in the Arctic.

While the approaches to derivation of the records (ice extent and ice type) are reasonable, the analysis of data quality, and the conclusions (and therefore the abstract) are rather qualitative and require some tightening up. If these data sets were to be presented as climate quality, then I should expect a more detailed assessment of the data quality and consistency (i.e., quantify the differences between the different time series and their trends). In particular:

Thanks for your review. We admit that the analysis and conclusions are rather qualitative – yet we hope they remain attractive. The purpose of the manuscript is not so much to make any extraordinary statements, but to consider the potential of the scatterometer record to address currently open research questions.

1. While I understand it is difficult to address the absolute uncertainties of these retrievals, I believe that the authors should at least address the potential variability in the estimates associated with the calibration of the scatterometers, especially since fixed thresholds are used in the separation of the ice classes.

Agreed. We have looked at the sensitivity of the scatterometer class extents to a fixed threshold uncertainty of 0.1 dB (associated to calibration accuracy). The results are plotted in Figure 12.

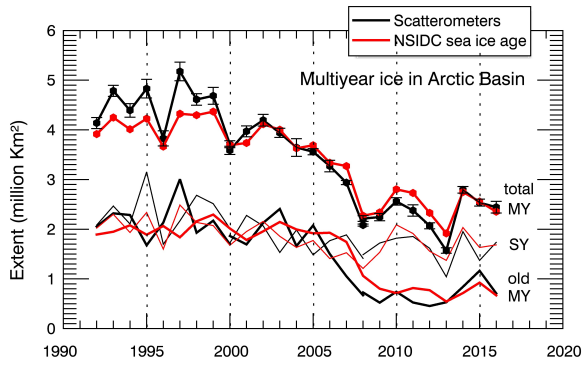

Figure 12: Time series of monthly wintertime (March) total multiyear sea ice extents (segmented into SY and older MY classes) within the Arctic Basin from the scatterometer (black) and the NSIDC sea ice age (red) records. Error bars are representative of the scatterometer class extent errors associated to a fixed backscatter threshold uncertainty of 0.1 dB (i.e. calibration accuracy).

2. Could the backscatter signature of SY ice just be a mixture of MY and FY-ice at the regional transition between the regions with the two dominant ice types?

Indeed, there is potential ambiguity there, particularly before 2007, which is problematic. It is the fact that SY ice appears as a separate mode in the backscatter histograms after 2007 (and not just as a transition between the FY and old MY clusters), along with the fact that it shows a spatial distribution similar to that provided by the NSIDC SY ice class, that encourages us to propose it as a separate entity.

We mention this uncertainty in Section 3.2: "From the analysis of joint backscatter distributions, we know that the scatterometer SY class is bound to contain varying amounts of FY-SY-MY mixtures, and probably some deformed FY too, thus an inherent ambiguity remains regarding the dominance of pure SY ice versus mixed FY-MY combinations in a cell labeled SY, particularly before 2007."

And address it again further below in Section 3.2: "The differentiation of SY and lower concentration of MY using a single frequency remains an open question though. By construction, the scatterometer SY class will accommodate various fractions of deformed FY and FY-SY-MY mixtures in it, which we suggest may be differentiated from the homogenous SY ice signature by recourse to dual Ku-band and C-band observations."

3. The authors' statement that: '...we find relative good agreement between the scatterometer SY ice class and the 2.0 m isoline from the ice thickness record, suggesting the utilization of the backscatter record as a reliable proxy for the estimation of thick sea ice thickness in the Arctic...' is not really supported by the analysis provided here. To demonstrate that the backscatter record is a proxy of thickness would entail more work.

For example, as an assessment, the authors could examine the mean ice thickness of the three ice types over the CryoSat-2 period and then examine the variability within the different categories. In any case, if the authors were to clarify what they meant by 'proxy' it would be more satisfactory.

Certainly. At this point, we cannot demonstrate but only suggest that the backscatter record should be tried as a proxy for the estimation of thick ice thickness (same as Tschudi et al., 2016, http://www.mdpi.com/2072-4292/8/6/457, using sea ice age). Further work along the lines suggested is currently under progress, but is considered out of the scope of this manuscript.

I think these issues should be addressed.

Reviewer 2

General comments:

The manuscript "A scatterometer record of sea ice extents and backscatter: 1992–2016" by Maria Belmonte Rivas et al.(tc-2018-68) introduces a data record of sea ice extent and backscatter merging different space-borne scatterometers (ERS, QuikSCAT, and ASCAT). In addition to presenting the methodology and resulting data record, the authors use the new almost 25 years long data to describe recent changes of Arctic sea ice observed after the September 2007 minimum. The contribution is generally of fair quality, and the text is understandable. The paper could be improved by giving some more details on the methodology, and discuss uncertainty of the retrievals.

A major concern are the shortcuts taken when comparing the capabilities of scatterometers (this study) versus (passive microwave) radiometers (e.g. NSIDC and OSISAF SIC data records), especially when it comes to summer melt. The claims of the authors on that specific topic are too often not supported by facts.
I encourage the authors to revise the way their findings are presented (not the methodology they apply to compute the data records) and to consider the comments below as an incentive to enhance the quality of their contribution. They should strive at being more balanced, and avoid shortcomings in the presentation of their results.

As a general comment: all the plots (especially the maps) are too small.

Thanks for the detailed revision of the manuscript and the many helpful suggestions, which we have strived to accommodate. We are confident in the superior sensitivity of the scatterometer sea ice extents to melting sea ice conditions, though the reviewer is correct in pointing out that melt ponding is neither the only nor the main reason behind SIE differences. We have certainly not investigated the relationship in detail, so the manuscript is arranged to clarify this point. Please see our replies below.

Specific comments:

1) Abstract: “providing a means to correct for summer melt ponding errors”. This is an overstatement. Unless you include in your study an investigation of the melt-pond season (May-June-July), for example using independent melt-pond fraction information (as done in Kern et al. 2017), the statement is not supported. You should be cautious with any statements about the alleged superiority of scatterometers to measure sea ice under melt-ponding conditions : the radar backscatter signal will be very much influenced by the surface water, and by the melting snow. In these conditions, it is hard to believe that scatterometers will have the accuracy to partition the 0%-30% reduced ice concentration (as measured by passive

microwave) into some percents of pure “open water” contribution and some percents of pure “melt water” contribution. Such a
partition however is what it would take to “provide a means to correct for summer melt ponding errors”.

Agreed. The sentence “providing a means to correct for summer melt ponding errors” has been removed. While we provide enough evidence (via validation against MODIS and SAR plates, to be found in the references) to support the superiority of scatterometers to measure sea ice under melting ice conditions, we do not provide any direct supporting evidence (yet?) of its relation to melt-ponding. A more extended commentary is provided as a reply to comment (22).

2) page 1 line 29: “instances of missing thin ice” ...from where is it missing? from the passive microwave records?

→ “but the precedent scatterometer records also feature instances of missing thin ice during the growth season”

3) page 2 line 5: when comparing sea ice estimates to operational ice charts, especially during summer, one should always question the accuracy of the charts.

Here we are only referring to results obtained by other groups. The validation of satellite sea ice extents admits a very limited set of choices, and operational ice charts are at this point one of the strongest. Direct validation against unambiguous SAR and MODIS scenes is probably better, though more tedious and limited in space and time. We understand the reviewer’s concern very well, so we make an effort to accommodate his/her comment:

→ “The validation of the summer sea ice extents from blended records against operational sea ice charts, whose accuracy during summer may also be arguable, shows negative biases by up to 30% (Aaboe et al., 2016), indicating that the distinct sea ice detection skills of scatterometer data may be lost in the blend.”

4) page 2 line 14 : “0.1 dB via buoy collocation” (do you mean “via collocation of wind retrievals at ocean buoy locations”?)

Agreed. The paragraph has been modified as suggested.

5) page 2 line 16 and 17: “which are known to cause discontinuities...”. please consider the following wording: “which -if not done properly- can affect long-term trends in sea ice concentration”. It is fortunate that the intercalibration of brightness temperatures is generally well taken care of by expert teams prior to computing data records of sea ice concentration. Titchner and Rayner (2014) discuss the stitching of SIC from different sources (passive microwave, navigational ice charts, etc..) and not the impact of non-optimal inter-calibration of passive microwave sensors can have on SIC trends.

Agreed. The paragraph has been modified as suggested.

6) page 2 offers a good occasion to re-state that passive microwave records are primarily aiming at mapping sea ice concentration, and sea ice extent is not a goal as such. Sea ice extent is only a downstream indicator.

This comment is accommodated:

→ "Note though, that the primary aim of passive microwave records is the mapping of sea ice concentration, sea ice extent being only a downstream indicator."

7) page 2 line 21: "It is known that...". Then please rather add a good citation.

Added a new citation:

Ulaby, F.T., Moore, R.K., and Fung, A.K.: Microwave Remote Sensing: Active and Passive, Volume III: From Theory To Applications, Artech House Publishers, London, UK, 1981.

8) page 3 line 4: when referring to the ice age data from NSIDC, a more recent citation is 10.1109/JSTARS.2010.2048305.

We added a new citation:

Tschudi, M.A., Fowler, C, Maslanik, J.A., Stroeve, J. 2010. Tracking the movement and changing surface characteristics of Arctic sea ice. *IEEE J. Selected Topics in Earth Obs. And Rem. Sens.*, 10.1109/JSTARS.2010.2048305.

9) page 3, line 20: which Metop platform(s) are used for ASCAT? please specify in the text.

→ "the Advanced Scatterometer (ASCAT) on Metop-A"

10) page 3 line 25: It would be useful to mention here the zenith angles of the different instrument (for example include here the first sentence of section 2.4).

Done – the first sentence of section 2.4 has been moved here.

11) page 3 line 25 : is it worth briefly mentioning NSCAT and why it was not selected in your data record?

NSCAT is a shorter-lived mission. While interesting in that it overlaps the ERS record, featuring collocated Ku and C-band data, its inclusion is envisioned for future extensions of the scatterometer record, along with the newer scatterometer data from ASCAT-B, ASCAT-C, OSCAT, Scatsat, HY, etc…

12) page 5, line 5: "stable wintertime backscatter levels" I understand this as your ice GMF is static, and not dynamically updated (e.g. with months). If I misunderstood, please consider making the sentence more explicit.

That is correct, the ice GMF is static, not dynamically updated.

13) page 6, line 13: please use one sentence to explain the difference in degrees of freedom.

Inserted a new sentence:

→ "The number of degrees of freedom is given by the difference between the size of the measurement space (N, or the number of looks provided by the instrument) and the size of the subspace occupied by backscatter points of a given class, allowing for a two-dimensional ocean wind GMF (wind cone) and a one-dimensional sea ice GMF (sea ice line)."

14) page 6, eq (7) : this is presented as the formula to compute daily estimates of the probabilities, thus supposedly gathering several passess of a given instrument. Yet, equation 7 does not show any indices. Could you make the indices appear in eq 7? Are the individual probabilities multiplied or averaged together?

The details are described in the references (Belmonte Rivas and Stoffelen, 2011; Belmonte Rivas et al., 2012; Otosaka et al., 2017). For completeness, we have inserted the sentence:

→ The *a priori* probabilities are updated at every pass using the previous pass posteriors as $p_0(ice) = p(ice|\sigma) = 1 - p_0(ocean)$, and relaxed towards uncertainty once a day.

15) page 6: it would be very interesting for the users to extend section 2.3 with some material to describe what would be your approach to *providing quantitative uncertainties*. A key discussion point might be how to treat that the PDFs of individual observations might be correlated with each others. To the least, uncertainties in the retrievals and how to quantify them should be discussed at the end of the manuscript.

Interesting question. The Bayesian probability already quantifies an uncertainty, whether a pixel belongs to the category of ocean winds, defined by the ocean GMF and its variance, or to the category of sea ice, defined by the sea ice GMF and its variance. In our opinion, quantifying the errors in the Bayesian inference is best left to validation against independent data (passive microwaves, MODIS and SAR plates, sea ice charts).

16) page 6: two informations are missing from section 2: 1) how do you define your SIE (from daily maps of sea ice probability...what is the threshold on probability?) and 2) describe in what sense "these algorithms have been tuned to match the passive microwave sea ice extents during the fall and winter months" (ref your page 2, line 11).

Thanks. We have inserted a new paragraph at the end of Section 2.3:

→ "Our Bayesian approach affords two parameters for tuning: one is the tolerance factor C_{mix} introduced in the sea ice model variance in Eq. (4), and the other is the probability threshold applied on the posterior in Eq. (7). With Quikscat, the tuning parameters have been adjusted empirically to match the passive microwave extents during the fall and winter months, and validated against an extensive series of SAR and MODIS plates during the spring and summer months (as described in Belmonte Rivas and Stoffelen, 2011), resulting in C_{mix} =3 and a 55% probability threshold to posterior sea ice probabilities. The Bayesian parameters for the ASCAT and ERS configurations have been adjusted similarly, and forced to remain consistent to the Quikscat extents across the mission overlaps periods, resulting in a seasonally varying C_{mix} for ASCAT with a 55% probability threshold, and a seasonally varying C_{mix} with a seasonally varying probability threshold ranging from 40% to 50% for ERS."

17) page 8 lines 9, 14, 15, 18: the use of "biases" is problematic as it implies you consider one source (the scatterometer?) is correct and the other (the passive microwave) is at an offset. Replace with "differences" at all 4 occasions.

All right. The paragraph has been modified as suggested.

18) page 8, lines 7-8 "the agreement... is of comparable high quality during the freezing season"... is it surprising? "these algorithms have been tuned to match the passive microwave sea ice extents during the fall and winter months" (ref your page 2, line 11).

A bit surprising, the tuning of the Bayesian algorithms (only using two parameters, C_{mix} and the probability threshold) seems to work very well.

19) Figure 7: are the colorbars for SIC correct? They would indicate that dark blue is for everything below 20%? It would be interesting to show contour lines of the sea ice extent from NSIDC-0051, OSI-430, and SCATT (e.g. on top of the NIC chart), as this is impossible to observe from the colored maps of SICs.

The colorbars for SIC are correct. The lower limits are 15% SIC for NSIDC-0051 and OSISAF-450 (top panels), and 55% probability for ASCAT (lower left panel). A comment regarding the lower limits has been inserted in the caption of Figure 7. The contour lines of the sea ice extent from NSIDC-0051, OSI-430 and SCAT have been overplotted on the NIC chart.

20) Concerning Figure 7: being an operational product meant for tactical navigation in the ice, the NIC ice charts are not a reference for accurate SIC monitoring. It uses active microwave data (SAR) that might suffer from exactly the same noise sources than the scatterometers, namely that scattered, faceted pieces of ice will seem brighter (higher backscatter) than if the corresponding area of ocean was covered by contiguous ice. Always question the accuracy of NIC charts (or other navigational ice charts), especially during summer.

Thank you for your comment. We are well aware of the ambiguities that make SAR image interpretation difficult. We are not so much concerned about the SIC accuracy of the NIC charts (SIC categories are very coarsely distributed in the NIC charts anyway), as with the fact that they also seem to capture more summer ice than passive microwaves (OSISAF or NSIDC) in a consistent manner.

21) Page 10: “surface wetness and melt ponding...during spring and summer [Comiso,...]” 1) consider also citing Kern et al. (2017) https://doi.org/10.5194/tc-10-2217-2016 as a more recent and quantitative assessment of the impact of melt-ponds on the passive microwave retrievals of SIC.

Agreed, added said citation.

22) Concerning Figure 6: it shows a mismatch between PMR and SCATT SIE for both hemispheres and the whole of spring+summer seasons, all the way until the SIE minimum. The sentences following Figure 6 (and Figure 7) point at “surface wetness and melt ponding” as a reason for the mismatch. This is not very intuitive, since:

1) the PMR SIE is defined as the area where SIC is larger than 15%. Although the impact of melt-ponding can be up to 20%-30% (Kern et al. 2017) at the maximum of the season, most of the melt-pond covered area will still show SIC>15%, thus only marginally influencing the PMR SIE.

   It is not unreasonable to think that melt ponding also affects the marginal sea ice.

2) Regardless of item 1), melt-ponding (on sea ice) is happening mostly in (late) May, June, and July, (early August) before they drain through the ice. There are no melt-ponds on top of sea ice in mid September (Figure 7). In addition, melt-ponds on top of sea ice are mostly (if not only) observed in the Arctic. Melt-ponds can thus not explain the SH mismatch you document.

[Rosel, Kaleschke and Birnbaum, TC, doi:10.5194/tc-6-431-2012] also show remarkable melt pond fractions in the Arctic in early September (see their Fig. 4). Certainly, we cannot say to what extent the SCAT to PMR SIE differences can be exclusively attributed to melt-ponding, as we provide no direct evidence to support a physical relationship - which nevertheless seems plausible.

However:

1) it is noted that the SCATT SIE has a finer spatial resolution than the SSM/I and SSMIS PMR SIE (this is obvious on Figure 7) due to the size of the FoVs of SSMIS at 19 and 37 GHz. Spatial resolution has been documented to have a definite influence on the SIE metric (Notz, 2014, https://www.the-cryosphere.net/8/229/2014/). Can spatial resolution have an influence on the SCATT SIE?

Generally, a higher grid resolution gives a lower sea-ice extent (Notz, 2014, https://www.the-cryosphere.net/8/229/2014/). So this effect is not likely to have much influence on the summer differences observed (with higher resolution scatterometers observing a larger sea ice extent than passive microwaves).

2) In the marginal ice zone, geometric scattering effects by disjoint, faceted ice floes will induce higher backscatter, and thus artificially enhanced radar "brightness" than if the same quantity of sea ice was present in a planar, contiguous way. The PMR signal is insensitive to these geometric effects. Could this geometric effect explain the difference in SIE you observe on Figure 6?

In our experience, most of the spring and summer errors along the ice margin (both in the NH and SH) involve darker surfaces such as shown in Figure 9B in (Belmonte Rivas and Stoffelen, 2011), which is suggestive of water saturated ice. For a more extended collection of evidence illustrating the nature of the SCAT to PMR summer differences using SAR and MODIS imagery, the reader is referred to the OSISAF visiting scientist report:

https://cdn.knmi.nl/system/data_center_publications/files/000/068/084/original/sea_ice_osi_saf_final_report.pdf?1495621021

3) Finally, if indeed your sea ice GMF is static and tuned for winter conditions (see page 5, line 5), then you should discuss if the spring+summer sea ice GMF is similar (than the winter one) so that to ensure that seasonality of the sea ice GMF does not artificially contribute to seasonality in SCATT SIE.

Back in the initial development stages, we did look at the seasonality in the distribution of sea ice backscatter measurements. The mode of the sea ice GMF remains essentially the same across the seasons, but in the spring and summer months, a large cloud of points is drawn towards the ocean GMF to form an extended tail of mixed sea ice and open ocean conditions. We did take care of this tail by introducing the tolerance C_{mix} parameter in Eq (4).

It is the (different degree of) inclusion of these mixed sea ice and open ocean conditions that is mainly responsible for the SCAT to PMR differences in the spring and summer months. Upon validation against SAR and MODIS plates (see the OSI-SAF report mentioned above), we learned that these mixed conditions include a variety of scenes, including low concentration ice (decaying sea ice floes), ice bands, brash (water saturated) ice, and mixtures thereof.

All in all, and as noted in the introduction to this review: the readability and impact of this paper would be greatly improved if 1) you described the observed differences between PMR and SCATT SIE without too hastily attributing them to deficiencies of the PMR SIEs (specifically melt-ponding), 2) you investigated (or pointed to earlier investigations) how other factors might explain (better?) the differences.

We provide ample evidence (in the references) to support the fact that observed differences between PMR and SCAT SIE indicate that SCAT is more sensitive to mixed sea ice and open ocean conditions (particularly prevalent in the spring and summer months) than PMR. The reviewer is correct in pointing out that melt ponding is neither the only nor the main reason behind SIE differences. We have certainly not investigated the relationship in detail, so the manuscript is arranged to clarify this point.

The paragraph (page 10, line 1) has been modified:

→"Surface wetness and melt ponding are thought to be responsible for large errors in passive microwave sea ice concentrations during spring and summer (Comiso and Kwok, 1996) (Kern et al, 2016), and these errors affect the ocean heat contents and associated surface fluxes when assimilated into ocean and atmosphere reanalyses (Hirahara et al., 2016). In this context, the scatterometer record nicely complements the passive microwave products in monitoring ~~the occurrence of melt ponding, and delineating~~ the expanse and evolution of the lower concentration and water-saturated (rotten) late spring and summer sea ice classes. It is the different degree of inclusion of these mixed sea ice and open ocean conditions that is mainly responsible for the sea ice extent differences observed between scatterometers and passive microwaves in the spring and summer months. The reader is referred to (OSISAF Visiting Scientist Report) for a more extended collection of collocated SAR and MODIS plates illustrating the nature of the differences observed in Figs. 5-6, which include a variety of scenes with decaying sea ice floes, ice bands, water saturated (brash) ice, and mixtures thereof."

OSISAF Visiting Scientist Report: https://cdn.knmi.nl/system/data_center_publications/files/000/068/084/original/sea_ice_osi_saf_final_report.pdf?1495621021

In the abstract (page1, line 12):

→ "… but shows higher sensitivity to lower concentration and melting sea ice during the spring and summer months~~, providing a means to correct for summer melt ponding errors~~."

In the conclusions (page 18, line 21)

→"In this context, the scatterometer sea ice extents and probabilities nicely complement the passive microwave products in providing a basis to monitor the occurrence of sea ice concentration errors due to ~~melt ponding~~ surface wetness, and to delineate the expanse and evolution of the rotten late spring and summer ice classes."

23) Figure 11: a legend/colorbar is missing. In addition the maps are too small (this applies to all figures in the draft manuscript). Figure 11 shows large discrepancies between the left and middle panels outside the central arctic ocean (e.g. second year ice in Bering Sea in 2008 for ASCAT but not QSCAT). Please either zoom your maps to the Arctic Basin (this is the area you discuss anyway, or comment the large discrepancies (how they can be mitigated).

Figure 11 has been enlarged, and a colorbar has been added.

For clarity, we introduced the following sentence:

→ "Outside of the red contour that delineates the Arctic basin mask in the left and middle panels of Figure 11, we cannot register older ice reliably because of the strong backscatter from deformed MIZ ice."

24) Page 15, line 18: as noted later in the text, the OSI-SAF product OSI-403 does not hold a MY ice concentration, but a MY/FY classification.

That is correct. The sentence is modified:

→ "The monthly averaged MY ice concentration for the month of March 2016 is calculated directly over the daily MY ice concentrations from the SICCI and Bremen products. Note that the OSISAF-403 is not a sea ice concentration product but a FY/MY classification. In this case, a daily MY concentration is defined (100% for the MY class, 50% for the ambiguous class, and 0% for the FY or OW classes) and a monthly average MY concentration is calculated as above. The monthly averaged sea ice age is calculated over the weekly NSIDC grids (using weeks 9 to 12) and over the daily SICCI grids, defining the SY ice class for a monthly averaged sea ice age between 1.5 and 2.5 years."

25) Figure 13: Several remarks:

1) the panels are too small.

   Now enlarged.

2) what date is this from (inside March 2016)? Or is this a monthly average for all panels? If a monthly average you should probably describe how the average is performed, given the variety of input variables (MYI conc, MYI classification, max SIA, mean SIA,...). It would make more sense to have a specific date.

   It is a monthly average, as stated in the caption. See our reply to comment (24) above.

3) consider adding coast lines.

   A coastal mask is already applied.

4) legend : the OSI-403 is not a MYI concentration product but a sea ice classification.

   See our reply to comment (24) above.

5) please add a "first year ice" color (or a sea ice edge line) on panels b) to f).

   Thanks for the suggestion. This figure discusses the representation multiyear ice. Adding a sea ice edge for FY would not help this purpose.

6) please check your plot c) and f) (from Korosov et al. 2017 data). If this is plotted from variable "sia" (the mean sea ice age), one has to look at 1<sia<2 for the second year ice (as soon as sia is > 1, then it has 2nd year ice contribution). The result will look much more similar to NSIDC SIA and the other maps, especially in the Beaufort Sea.

We checked the plots after redefining the SY class using a monthly averaged SIA between 1 and 2 years, as suggested. The problem with the apparently missing SY ice over the Beaufort Sea in the SICCI product is not related to the SIA, but related to the MYI concentration, which is lower than 30% - thus masked in the figure.

7) the description of the location of the features is difficult to follow in the text, would it be an idea to write letters on the map (A, B, C, ...) and refer to them?

Agreed and done.

8) all estimates (but yours in a) show a thin tongue of older ice extending across the Arctic Ocean towards the New Siberian Islands. It can even be noticed somewhat in the Cryosat-2 thickness. It is visible on the shades of "normalized backscatter" in your panel a). Given the variety of methods used for all other panels, are you confident that your new estimate in a) is correct and that there is no such tongue of older ice? Discuss.

Good point. We pondered over this feature at length, and it does justice to mention it.

→ "Another interesting feature refers to the thin tongue of older ice extending across the Arctic Basin towards the New Siberian Islands (see label D in Fig. 13g), which is seen by all products, even faintly in the AWI sea ice thickness, but falls below the SY threshold in the scatterometer-based MY ice classification. We cannot offer an explanation for this feature at the moment, other than acknowledging that efforts towards ensuring the consistency among MY ice products in the Arctic should warrant further research."

26) Page 17, line 15 : "as verified by comparison to NIC sea ice charts". NIC sea ice charts are not the truth. Please use a different wording than "verify"..

→ "… but show enhanced sensitivity to lower concentration and water-saturated sea ice conditions during the spring and summer months, as verified by numerous comparisons to MODIS and SAR imagery."

27) Page 17, line 18 : "typically underestimating the summer sea ice concentration and summer sea ice extent by up to 30%". Which one? SIC or SIE? As discussed above an underestimation of high SICs, even by 30% will have limited impact on the SIE (defined as SIC>15%). Rewrite

We have cited a number of references reporting estimates of PMR SIC and SIE errors up to 30% in the summer. Another comparison (OSISAF 403 against NIC charts in the SH) here:

http://osisaf.met.no/validation/img/sh_edge_bar_plot_full.png

28) page 17, line 21: “providing a solid basis to monitor the occurrence of sea ice concentration errors due to melt ponding”. NO. See notes from the introduction. Rewrite.

Agreed. This sentence has been removed; please see our reply to comment (22) above.

29) page 17, line 29, 30: this sentence is an exact copy-paste from previous section. Avoid word-by-word repeats, please.

Thanks for the suggestion. This sentence has been reworded into:

→ “Monitoring the evolution of the complementary old MY and SY classes shows that the decline in the total MYI ice extent observed in the Arctic has been driven by loss of old MY ice, while the more steady production of SY ice has been acting to stabilize those losses, contributing to later recovery events such as observed in 2014.”

30) page 18, line 15 : to use Sea Ice Type (or Age) as a proxy for Sea Ice Thickness is not a new idea. It would be good to cite earlier attempts e.g. Tschudi et al. 2016, http://www.mdpi.com/2072-4292/8/6/457.

Thanks for the suggestion. A new citation has been inserted (page 16, line 10):

Tschudi, M.A., Stroeve, J. and Stewart, J.S.: Relating the age of Arctic sea ice to its thickness, as measured during NASA’s ICEsat and IceBridge, *Remote Sens.* **2016**, *8*(6), 457; https://doi.org/10.3390/rs8060457 , 2016.

Technical corrections:

31) page 1 line 14: “record sea ice loss” : consider another term than “record” as it is used elsewhere in the paper (including the abstract) as “data record”.

→ “historical sea ice loss”

32) page 1 line 19: “1978” (with the start of SMMR in Oct 1978). There are passive microwave instruments before (e.g. ESMR), but the routine monitoring indeed starts in 1978 with SMMR.

→ “1978”

33) page 3 line 22: “mission transition periods”.. consider “mission overlap periods”

→ “mission overlap periods”

34) page 3, line 13; “measurements about extended”...do you mean “around”?

→ “measurements around extended”

35) Figure 4: please add a second legend with solid line for NH and dashed line for SH.

Done.

36) Figure 5: please add text in the plot area for NH (top) and SH (bottom).

Done.

37) page 7, line 15 : you are probably referring to OSI-430, that extends OSI-409a (http://osisaf.met.no/p/ice/index.html#conc-reproc). Same in caption to Figure 7.

That is correct, OSI-430. We have amended the typo, both in text and caption.

38) page 8, line 9 : “Quikscat-to-ERS”... you probably mean “ERS-Quikscat”?

That is correct → “ERS-to-Quikscat”

39) Figure 6: you seem to have a dip in QuikSCAT SIE in antarctic curve for 2000 (around day 260).

It is a dip in the Antarctic OSISAF0-409a SIE curve. We checked the daily OSISAF 409a maps around the suggested date, but did not find anything strange (i.e. it does not seem to be an instrumental artifact…)

40) page 10, line 24: “arrival of summer signatures” consider “appearance of summer signatures”?

→ “appearance of summer signatures”

A scatterometer record of sea ice extents and backscatter: 1992-2016

Maria Belmonte Rivas[1,3], Ines Otosaka[1,2], Ad Stoffelen[1], Anton Verhoef[1]

[1]Royal Netherlands Meteorology Institute (KNMI), de Bilt, 3731 GA, The Netherlands
[2]Center for Polar Observation and Modelling (CPOM), University of Leeds, Leeds, LS2 9JT, United Kingdom
[3]Instituto de Ciencias del Mar (ICM), Consejo Superior de Investigaciones Cientificas (CSIC), 08003, Barcelona, Spain

Correspondence to: Maria Belmonte Rivas (belmonte@knmi.nl)

Abstract. This paper presents the first long-term climate data record of sea ice extents and backscatter derived from inter-calibrated satellite scatterometer missions (ERS, QuikSCAT and ASCAT) extending from 1992 to present date. This record provides a valuable independent account of the evolution of Arctic and Antarctic sea ice extents, one that is in excellent agreement with the passive microwave records during the fall and winter months but shows higher sensitivity to lower concentration and melting sea ice during the spring and summer months. The scatterometer record also provides a depiction of sea ice backscatter at C and Ku-band, allowing the separation of seasonal and perennial sea ice in the Arctic, and further differentiation between second year (SY) and older multiyear (MY) ice classes, revealing the emergence of SY ice as the dominant perennial ice type after the historical sea ice loss in 2007, and bearing new evidence on the loss of multiyear ice in the Arctic over the last 25 years. The relative good agreement between the backscatter-based sea ice (FY, SY and older MY) classes and the ice thickness record from Cryosat suggests its applicability as a reliable proxy in the historical reconstruction of sea ice thickness in the Arctic.

Maria Belmonte Rivas 17/7/2018 17:57
Deleted: , providing a means to correct for summer melt ponding errors.

Maria Belmonte Rivas 17/7/2018 17:57
Deleted: record

1 Introduction

Dating as far back as 1978, passive microwave sensors provide the longest record of sea ice concentration and extents available to date, and are currently established as the sea ice monitoring standard for climate studies, regardless of well-known difficulties around the detection of lower concentration and melting sea ice conditions during the summer months (Meier et al., 2015). The scatterometer sea ice record presented here only dates back as far as 1992, but proves more sensitive to summer sea ice, its primary purpose being the conservative detection and removal of ice contaminated scenes that compromise scatterometer wind retrievals. Previous long-term scatterometer sea ice records have been developed spanning the decade-long QuikSCAT mission from 1999 to 2009 (Remund and Long, 2014), and extended into 2014 using the Oceansat-2 scatterometer (OSCAT) mission (Hill and Long, 2017). These precedent scatterometer records (which use maximum likelihood class discrimination based on the Ku-band pseudo-polarization HH/VV ratio and other parameters) already underline the presence of negative biases in passive microwave sea ice extents during the melt season, but they also feature instances of missing thin ice during the growth season (Meier and Stroeve, 2008).

Maria Belmonte Rivas 17/7/2018 17:57
Deleted: 1979

Some research groups have opted to blend active and passive microwave observations (i.e. the gradient and polarization ratios from radiometer, along with the C-band anisotropy coefficient from scatterometer data) in a multi-sensor approach towards a sea ice edge product (Aaboe, Breivik and Eastwood, 2015). The validation of the summer sea ice extents from blended records against operational sea ice charts, whose accuracy during summer may also be arguable, shows negative biases by up to 30% (Aaboe et al., 2016), indicating that the distinct sea ice detection skills of scatterometer data may be lost in the blend. Note though, that the primary aim of passive microwave records is the mapping of sea ice concentration, sea ice extent being only a downstream indicator.

In this paper, an independent record of sea ice extents has been produced from inter-calibrated scatterometer data: the QuikSCAT mission from 1999 to 2009 (Belmonte Rivas and Stoffelen, 2011), extended forward to present day with the ASCAT record (Belmonte Rivas et al., 2012), and backwards to 1992 with the ERS mission (Otosaka et al., 2017), using dedicated Bayesian sea ice detection algorithms designed to maximize the skill for ocean/ice discrimination. These algorithms have been tuned to match the passive microwave sea ice extents during the fall and winter months, and to remain consistent across the scatterometer overlap periods in 2000 (ERS with QuikSCAT) and 2008 (QuikSCAT with ASCAT). The stability and inter-calibration of the ERS, QuikSCAT and ASCAT backscatter records is guaranteed to within 0.1 dB via buoy collocation (QuikSCAT; Verhoef and Stoffelen, 2016), ocean calibration (ASCAT and ERS; Verhoef and Stoffelen, 2017) and nonlinear corrections from cone metrics (ERS; Belmonte Rivas et al, 2017), offering a stable reference to verify the consistency of calibration adjustments made in passive microwave records, which –if not done properly- are known to cause discontinuities and affect long-term trends in sea ice concentration (Eisenman, Meier and Norris, 2014) (Titchner and Rayner, 2014).

The scatterometer sea ice record also monitors the evolution of sea ice backscatter collected at C-band and Ku-band, which are widely applied to discriminate ice classes, such as first year (FY) and older (second year SY, and multiyear MY) sea ice in the Arctic. It is known that sea ice backscatter is modulated by surface permittivity, surface roughness and the presence of volume inhomogeneities, such as air and brine pockets, or snow layers above (Ulaby, Moore and Fung, 1981). The main basis for FY/MY ice separation lies in older ice types becoming brighter with increased volume scattering after summer melt, although MY detection may become difficult by patches of bright FY ice that may have locally undergone deformation. To date, the separation between Arctic FY and MY ice types using active microwaves has relied on fixed backscatter thresholds defined after visual inspection of stable winter backscatter histograms. For example, (Kwok, 2004) established -14.5 dB as an optimal threshold for the QuikSCAT Ku-band VV polarized measurements based on visual examination of the subjective FY and MY ice boundaries in combined winter data sets of QuikSCAT and C-band SAR from RADARSAT. Other than calibration issues, the main problem with the fixed-threshold approach is the seasonal variability of the FY-MY backscatter signatures, along with sensitivity to deformed FY ice types or a developing snow cover. On the other hand, the classification of sea ice types using passive microwaves (Gloersen and Cavalieri, 1986; Comiso, 2012) has relied

Maria Belmonte Rivas 17/7/2018 17:57
Deleted: However,

Maria Belmonte Rivas 17/7/2018 17:57
Deleted: are still negatively biased in the summer relative to

Maria Belmonte Rivas 17/7/2018 17:57
Deleted: .

on the spectral gradient and polarization signatures of sea ice brightness temperatures (with MY surfaces featuring more negative spectral gradients and lower polarization than FY ice, along with lower emissivities). The spatial and temporal distributions of perennial ice derived from passive microwaves in the Arctic have been shown to differ somewhat from those of SAR (Kwok, Comiso and Cunningham, 1996), their differences depending on atmospheric conditions and processes that affect the ice temperature and emissivity in ways that contribute to apparent concentration changes (Thomas, 1993). According to the IPCC AR5, the rate of decline in the extent of multiyear ice observed by both passive and active microwaves is consistent with the decline of old ice types estimated from the analysis of ice drift by (Maslanik et al., 2007) (Tschudi et al, 2010), confirming that the Arctic has lost much of its thicker ice. Still differences remain between scatterometer and radiometer multiyear ice extents (Comiso, 2012) associated to different sensitivities to sea ice type and snow cover, which should be better understood.

The introduction of an inter-calibrated sea ice extent and backscatter record from multiple scatterometer missions (ERS, QuikSCAT, ASCAT) consistently connected from 1992 to 2016 through dedicated and validated sea ice detection and backscatter normalization algorithms is the object of this contribution. In Section 2, we introduce the satellite scatterometer missions and the Bayesian detection algorithms that constitute this record. In Section 3, the scatterometer sea ice extents are compared against passive microwave fields, showcasing their agreement and distinct sensitivities. This section also provides an overview of the long-term evolution of sea ice extents and sea ice types afforded by 25 years of scatterometer data, along with a taste of its potential to stimulate new research questions.

2 Satellite scatterometer missions

The continuous monitoring of the Polar Regions with satellite scatterometers began in March 1992 after the launch of the European Remote Sensing (ERS) satellites, which operated a C-band instrument (5.3 GHz, VV polarization) in global mode until January 2001. It was continued on July 1999 by the Quick Scatterometer (QuikSCAT), which operated a Ku-band instrument (13.4 GHz, HH and VV polarization) up until November 2009. The scatterometer record ends with another C-band instrument that collects VV polarized backscatter at 5.3 GHz, the Advanced Scatterometer (ASCAT) on Metop-A, operating from January 2007 to the present date. The temporal spans of the satellite missions that make up the scatterometer record are illustrated in Fig. 1, showing the location of the mission overlap periods (2000 and 2008) used to verify the consistency of the sea ice extents and sea ice types across the C and Ku-band missions. For reference, the observation geometries of the constitutive ERS, QuikSCAT and ASCAT scatterometers (namely, three single-sided VV polarization fan-beams, single rotating VV and HH polarization pencil beams, and three double-sided fan-beams, respectively) are shown in Fig. 2. While the QuikSCAT mission observes backscatter at Ku-band from an incidence angle of 54 deg (outer VV-pol beam) and 46 deg (inner HH-pol beam), the ERS and ASCAT missions observe backscatter at C-band from a broad range of incidence angles collected across the swath (from 18 to 64 deg in VV-pol).

Maria Belmonte Rivas 17/7/2018 17:57
Deleted:),

Maria Belmonte Rivas 17/7/2018 17:57
Deleted: transition

Maria Belmonte Rivas 17/7/2018 17:57
Moved (insertion) [1]

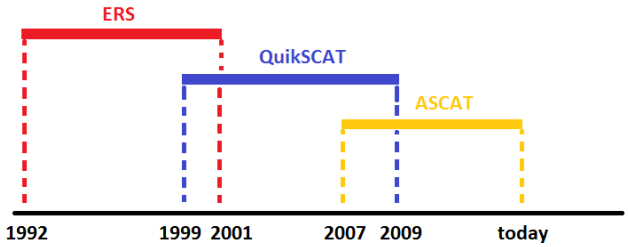

Figure 1: Temporal spans of the satellite scatterometer missions used.

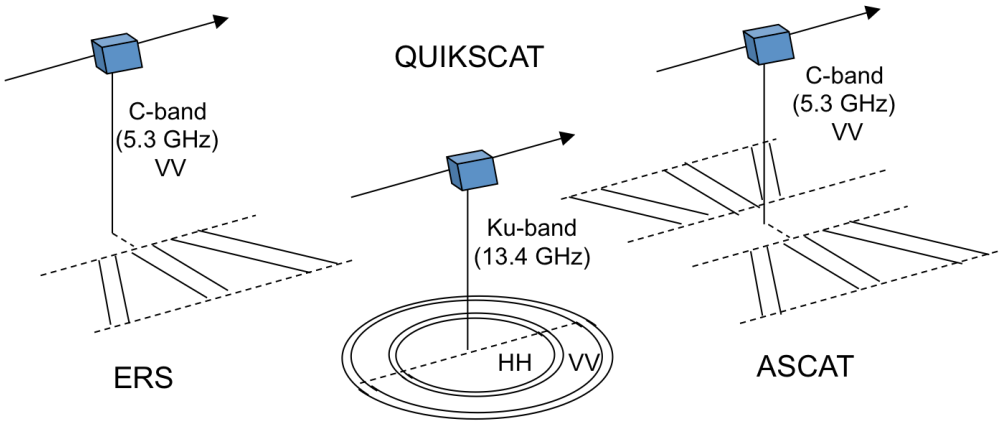

Figure 2: Observation geometries of the satellite scatterometers.

5

2.1 Sea ice detection with scatterometers

The algorithm for sea ice detection with scatterometers is a maximum likelihood class discrimination approach based on probabilistic distances to ocean wind and sea ice geophysical model functions (GMFs). The GMFs describe the behaviour of backscatter as a function of observation geometry (i.e., incidence and azimuth angles) and geophysical variables such as
10 wind speed and direction, or sea ice type.

2.2 Geophysical model functions

The ocean wind GMF, also known as the wind cone, is an empirically derived model used to derive ocean surface wind vectors operationally (see Fig. 3): we presently use CMOD7.1 (Stoffelen et al., 2017) for ERS and ASCAT, and NSCAT-4 (Verhoef and Stoffelen, 2017) for QuikSCAT. The sea ice GMF, also known as the sea ice line, is empirically derived from stable wintertime backscatter levels (Belmonte Rivas and Stoffelen, 2011; Belmonte Rivas et al., 2012; Otosaka et al., 2017). Physically, the discrimination between open water and sea ice classes is based on the separability between surface and volume scattering effects: in the QuikSCAT case, the discrimination relies on polarization and azimuthal anisotropy of backscatter (high for open water; lower for sea ice), while in the ERS/ASCAT case, the discrimination relies on backscatter directivity (i.e. the derivative of backscatter with incidence angle) and azimuthal anisotropy (high for open water; lower for sea ice). Previous Bayesian formulations for sea ice detection with scatterometer data, e.g., (Remund and Long, 2014), have used aggregates such as mean backscatter, polarization ratio and azimuthal anisotropy as class discriminants, and empirically adjusted covariances to represent the class dispersions. The advantage of the GMF approach is that the dispersion of measurements around extended class model functions is smaller than about class aggregate means, approaching the limits imposed by the scatterometer noise levels, and allowing the Bayesian method to reach its maximum discrimination power (Otosaka et al., 2017).

Maria Belmonte Rivas 17/7/2018 17:57
Deleted: about

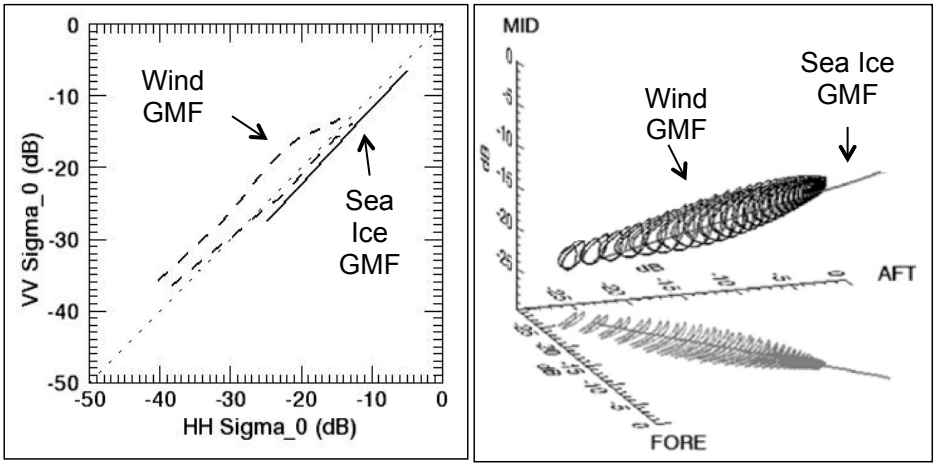

Figure 3: Ocean wind and sea ice Geophysical Model Functions (GMFs) in the scatterometer measurement space: QuikSCAT (left) and ERS/ASCAT (right). Plots adapted from (Belmonte Rivas and Stoffelen, 2011; Belmonte Rivas et al., 2012)

2.3 Bayesian sea ice probability

To calculate the Bayesian sea ice probability, the algorithm computes the minimum normalized squared distance (or maximum likelihood estimator, MLE) from observations σ_i^0 to the sea ice σ_{ice}^0 and ocean wind σ_{ocean}^0 model functions:

$$MLE_{ocean} = \sum_{i=1,\dots,N}\left(\sigma_i^0 - \sigma_{ocean,i}^0\right)^2 / var[\sigma_{ocean,i}^0] \quad (1)$$

$$MLE_{ice} = \sum_{i=1,\dots,N}\left(\sigma_i^0 - \sigma_{ice,i}^0\right)^2 / var[\sigma_{ice,i}^0] \quad (2)$$

where N is the number of instrument looks (N=4 for QuikSCAT, N=3 for ERS/ASCAT) and the model variances describe the tolerable (statistical average) range of departures to the GMF:

$$var[\sigma_{ocean}^0] = \left(K_p^2 + K_{geo}^2\right)\sigma_{ocean}^{0\ 2} \quad (3)$$

$$var[\sigma_{ice}^0] = \left(C_{mix} K_p \sigma_{ice}^0\right)^2 \quad (4)$$

where K_p represents instrumental noise, K_{geo} is a measure of backscatter variability due to wind variability within the sensor footprint, and C_{mix} is a tolerance factor introduced in the sea ice model variance to allow for backscatter variability introduced by mixed open water and sea ice conditions. The conditional open water and sea ice probabilities are represented by chi-square distributions with N-1 and N-2 degrees of freedom for the sea ice and ocean wind classes:

$$p(MLE_{ice}) = \chi^2_{N-1}(MLE_{ice}) \quad (5)$$

$$p(MLE_{ocean}) = \chi^2_{N-2}(MLE_{ocean}) \quad (6)$$

The number of degrees of freedom is given by the difference between the size of the measurement space (N, or the number of looks provided by the instrument) and the size of the subspace occupied by backscatter points of a given class, allowing for a two-dimensional ocean wind GMF (wind cone) and a one-dimensional sea ice GMF (sea ice line). The Bayesian sea ice *posterior* probability is finally calculated as:

$$p(ice|\sigma) = \frac{p(\sigma|ice)p_0(ice)}{p(\sigma|ice)p_0(ice)+p(\sigma|ocean)p_0(ocean)}, \quad (7)$$

where $p_0(ice)$ and $p_0(ocean)$ are *a priori* probabilities derived from previous observations, and $p(\sigma|ice)$ and $p(\sigma|ocean)$ are the conditional open water and sea ice probabilities defined in Eqs. (5-6). The *a priori* probabilities are updated at every pass using the previous pass posterior as $p_0(ice) = p(ice|\sigma) = 1 - p_0(ocean)$, and relaxed towards uncertainty once a day. In principle, we do not grant any statistical relation between sea ice probability and sea ice concentration.

Our Bayesian approach affords two parameters for algorithmic tuning: one is the tolerance factor C_{mix} introduced in the sea ice model variance in Eq. (4), and the other is the probability threshold applied on the posterior in Eq. (7). With Quikscat, the tuning parameters have been adjusted empirically to match the passive microwave extents during the fall and winter months, and verified extensively against SAR and MODIS imagery during the spring and summer months (Belmonte Rivas and

Maria Belmonte Rivas 17/7/2018 17:57
Deleted: And the daily Bayesian sea ice

Maria Belmonte Rivas 17/7/2018 17:57
Formatted: Font:+Theme Body, Font color: Text 1

Maria Belmonte Rivas 17/7/2018 17:57
Deleted: the

Maria Belmonte Rivas 17/7/2018 17:57
Formatted: Space Before: 0 pt, After: 0 pt

Stoffelen, 2011), resulting in C_{mix} =3 and a 55% probability threshold to posterior sea ice probabilities. The Bayesian parameters for the ASCAT and ERS configurations have been adjusted similarly, and forced to remain consistent to the Quikscat extents across the mission overlaps periods in 2000 and 2008, resulting in a seasonally varying C_{mix} for ASCAT with a 55% probability threshold, and a seasonally varying C_{mix} with a seasonally varying probability threshold ranging from 40% to 50% for ERS.

2.4 Normalized sea ice backscatter

In order to build a uniform record of sea ice backscatter, all the C-band measurements must be normalized to a standard incidence angle (chosen 52.8 deg, set in the middle of the ASCAT mid-beam swath, and closest to the QuikSCAT VV-pol incidence) using a model that describes the dependence of C-band sea ice backscatter on incidence angle. In the present version, the normalization assumes a linear relation between C-band backscatter and incidence angle using sea ice type dependent coefficients (Ezraty and Cavanie, 1999). A refined incidence angle correction based on the empirical C-band sea ice backscatter model developed in (Otosaka et al., 2017) is planned for a future release. The largest obstacle, though, arises from the presence of composite C and Ku-band observations in a single backscatter record, since their sensitivities to sea ice type differ. Both frequencies are similarly responsive to surface roughness, e.g., over deformed first year sea ice, but Ku-band is more responsive to volume scattering in multiyear ice (Ezraty and Cavanie, 1999). As a result, the separability between deformed FY and MY ice classes is better at Ku-band. At C-band, the disambiguation between deformed FY and MY ice classes is more difficult in terms of backscatter alone, although recourse can always be made to additional information, such as the monitoring of backscatter derivatives, or the introduction of geographical constraints, such as a marginal sea mask.

Maria Belmonte Rivas 17/7/2018 17:57
Moved up [1]: While the QuikSCAT mission observes backscatter at Ku-band from an incidence angle of 54 deg (outer VV-pol beam) and 46 deg (inner HH-pol beam), the ERS and ASCAT missions observe backscatter at C-band from a broad range of incidence angles collected across the swath (from 18 to 64 deg in VV-pol).

Maria Belmonte Rivas 17/7/2018 17:57
Deleted:

3 Historical record

3.1 Sea ice extents

The time series of Arctic and Antarctic sea ice extents observed by the ERS, ASCAT and Quikscat scatterometers from 1992 to 2016 are shown in Fig. 4, along with the differences to the sea ice extents from the SSMI(S) passive microwave sea ice concentration (15% threshold) algorithms from the NSIDC-0051 (Cavalieri et al., 2015) and the OSISAF's latest major reprocessing release [OSISAF-409a as in (Tonboe et al, 2015) extended into 2016 with OSISAF-430] in Fig. 5. The sea ice extents are constrained by a unique land mask built from the union of all active and passive sensors' land masks. No significant long-term trends are observed in the active-to-passive differences, other than a slight increase in the variability of the Arctic sea ice extent biases from 1992 to 1996, which has been attributed to data gaps in the ERS-1 mission due to SAR operations (Otosaka et al., 2017).

Maria Belmonte Rivas 17/7/2018 17:57
Deleted: 450

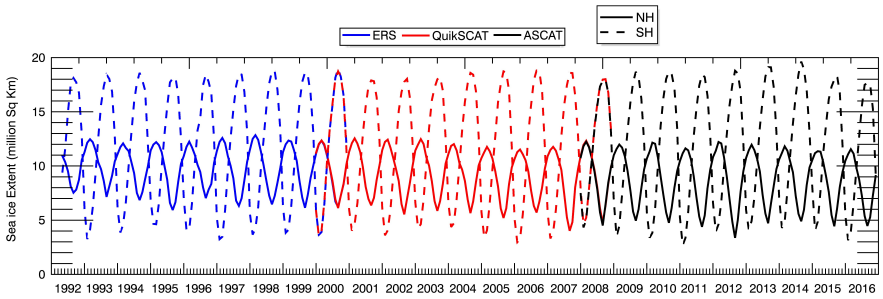

Figure 4: Time series of monthly Arctic (continuous) and Antarctic (dashed) scatterometer sea ice extents from 1992 to 2016.

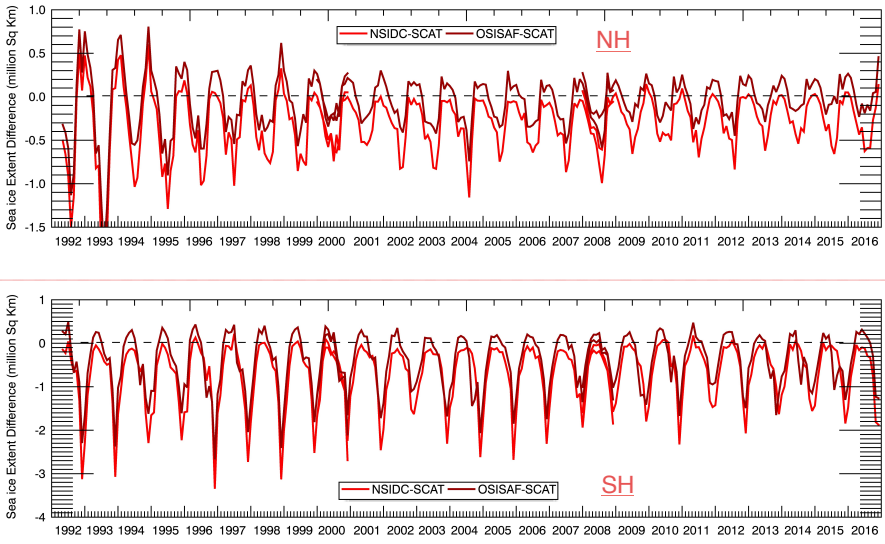

Figure 5: Time series of scatterometer sea ice extent differences to passive microwave (SSMI-based) products from NSIDC-0051 and OSISAF-409a from 1992 to 2016 for the Arctic (top) and Antarctic (bottom).

The correspondence between the Quikscat scatterometer and passive microwave sea ice extents from the NSIDC (NT-based) algorithms has been extensively verified using coincident SAR imagery (Belmonte Rivas and Stoffelen, 2011) to reveal excellent agreement during the winter and fall seasons, and persistent differences during the spring and summer months.

Maria Belmonte Rivas 17/7/2018 17:57

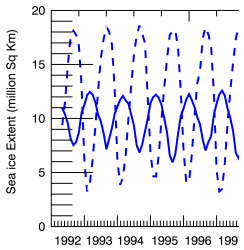

Deleted:

Maria Belmonte Rivas 17/7/2018 17:57

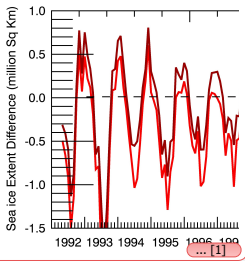

Deleted:

Figure 6 illustrates the seasonal pattern of active-to-passive sea ice extent differences over the ERS/Quikscat and Quikscat/ASCAT overlap periods in 2000 and 2008. The agreement between the overlapping C and Ku-band scatterometer sea ice extents is very good all year round, with differences within 0.25 million km^2 and an estimated ice edge accuracy of about 20 km. The agreement between the scatterometer and passive microwave sea ice extents is of comparable high quality during the freezing season, but diminishes during the melting (spring and summer) months, noting that the amplitude of summer differences to the OSISAF-409a product is smaller than the the NSIDC-0051 product, particularly for the Arctic sea ice extents. The largest sea ice extent differences occur at the end of the summer, reaching from 0.6 to 2.0 million km^2, and corresponding to estimates of the minimum sea ice extent that may differ by up to 10-30%. As a result, the expression of the Arctic minimum sea ice extent in the scatterometer record may occur up to 15 days later than with passive microwaves. Figure 7 illustrates a typical spatial layout of active-to-passive sea ice extent biases for a particular late summer day (15th September 2016). The collocated NIC chart for this particular day, which delineates the subjective extent of the summer sea ice pack (with sea ice concentrations larger than 80% and marginal sea ice excluded), showcases the higher sensitivity of the scatterometer record to lower concentration and water-saturated sea ice conditions, particularly over the confluence of the Chukchi and East Siberian Seas, along with the large differences in sea ice concentration estimates from different passive microwave algorithms (of up to 30%) in the central Arctic (Ivanova et al., 2015).

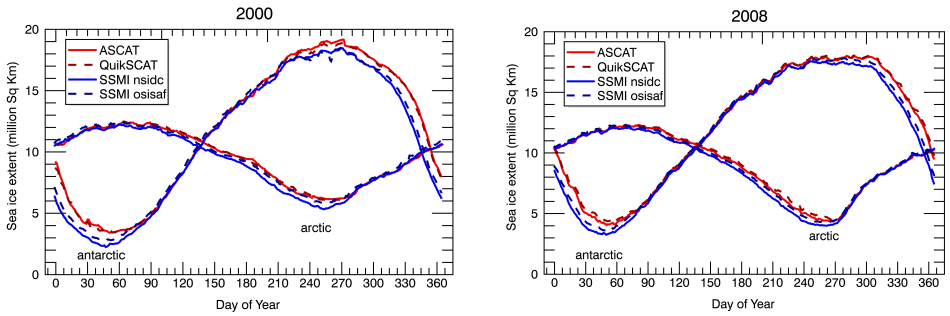

Figure 6: Comparison of ERS, QuikSCAT, ASCAT and passive microwave (OSISAF-409a and NSIDC-0051) sea ice extents over 2000 (left) and 2008 (right).

Maria Belmonte Rivas 17/7/2018 17:57
Deleted: biases

Maria Belmonte Rivas 17/7/2018 17:57
Deleted: -to-ERS

Maria Belmonte Rivas 17/7/2018 17:57
Deleted: -to-

Maria Belmonte Rivas 17/7/2018 17:57
Deleted: transition

Maria Belmonte Rivas 17/7/2018 17:57
Deleted: biases in

Maria Belmonte Rivas 17/7/2018 17:57
Deleted: in

Maria Belmonte Rivas 17/7/2018 17:57
Deleted: biases

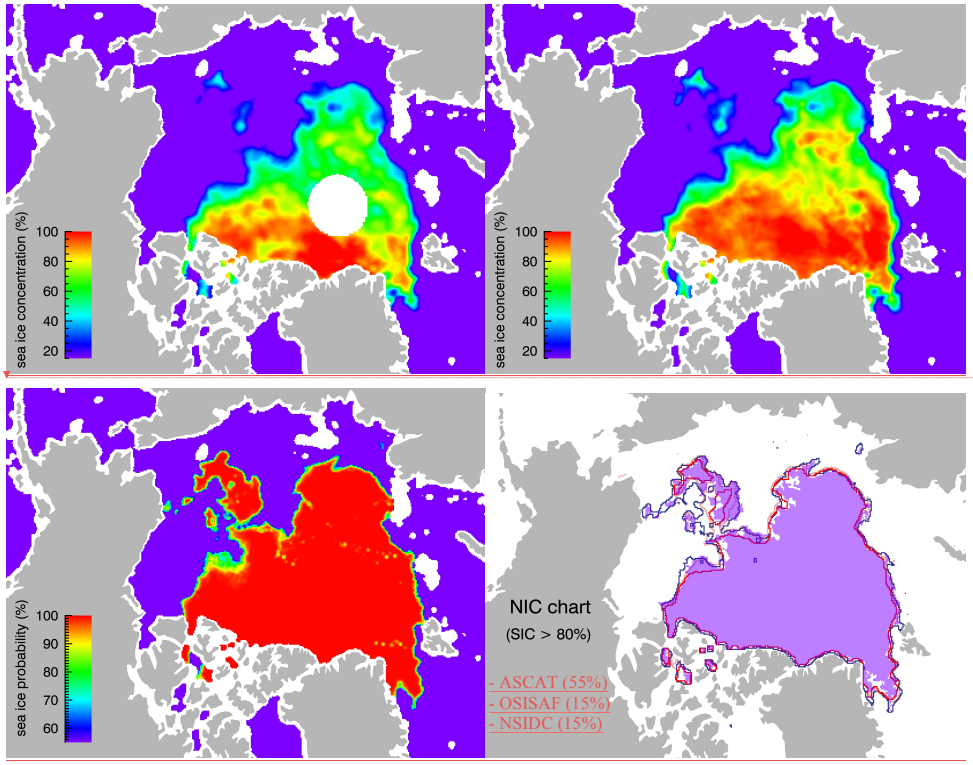

Figure 7: Comparison of summer sea ice extents on September 15th 2016 from passive microwaves (NSIDC-0051 top left, OSISAF-430 top right), active microwaves (ASCAT, bottom left) and NIC sea ice charts (bottom right). The color scales represent sea ice concentration (top panels, lower limit 15%), sea ice probability (bottom left panel, lower limit 55%) and NIC sea ice concentration larger than 80%.

Surface wetness and melt ponding are thought to be responsible for large errors in passive microwave sea ice concentrations during spring and summer (Comiso and Kwok, 1996) (Kern et al, 2016), and these errors affect the ocean heat contents and associated surface fluxes when assimilated into ocean and atmosphere reanalyses (Hirahara et al., 2016). In this context, the scatterometer record nicely complements the passive microwave products in monitoring the expanse and evolution of the lower concentration and water saturated (rotten) late spring and summer sea ice classes. It is the different degree of inclusion of these mixed sea ice and open ocean conditions that is mainly responsible for the sea ice extent differences observed

Maria Belmonte Rivas 17/7/2018 17:57
Deleted:
... [2]

Maria Belmonte Rivas 17/7/2018 17:57
Deleted: 450

Maria Belmonte Rivas 17/7/2018 17:57
Deleted:),

Maria Belmonte Rivas 17/7/2018 17:57
Deleted: probabliity

Maria Belmonte Rivas 17/7/2018 17:57
Deleted:)

Maria Belmonte Rivas 17/7/2018 17:57
Deleted: [

Maria Belmonte Rivas 17/7/2018 17:57
Deleted:],

Maria Belmonte Rivas 17/7/2018 17:57
Deleted: [

Maria Belmonte Rivas 17/7/2018 17:57
Deleted:].

Maria Belmonte Rivas 17/7/2018 17:57
Deleted: occurrence of melt ponding, and delineating the expanse and evolution of the rotten late summer ice classes.

between scatterometers and passive microwaves in the spring and summer months. The reader is referred to (Belmonte Rivas and Stoffelen, 2009) for a more extended collection of collocated SAR and MODIS plates illustrating the nature of these differences, including a variety of scenes dominated by water saturated (brash) ice, decaying floes, ice bands, and mixtures thereof.

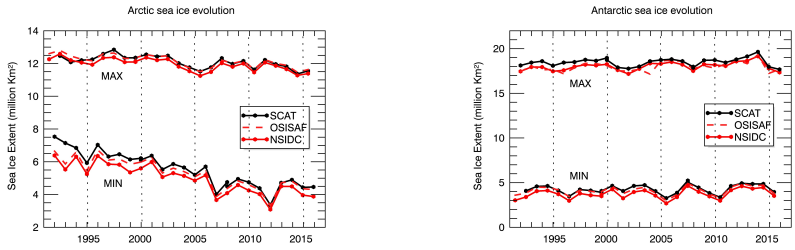

Figure 8: Evolution of minimum and maximum monthly sea ice extents from scatterometers (black line) and passive microwaves (continuous and dashed red lines) from 1992 to 2016 for the Arctic (left) and Antartic (right).

Figure 8 shows the long-term evolution and inter-annual variability of the Arctic and Antarctic minimum and maximum sea ice extents from the scatterometer and passive microwave records. These figures attest to the coincident emergence of significant events, such as the Arctic summer minima in 2007 and 2012, or the Antarctic wintertime maxima in 2014, on top of long-term trends that bear witness to Arctic sea ice decline, and a modest increase in Antarctic sea ice extents. Note that while the NSIDC algorithm ranked the summer of 2016 as second lowest in Arctic sea ice extent, tied with 2007 (NSIDC, 2016), the scatterometer record observes a somewhat slower trend in the decline of Arctic summer ice over the last 5 years, and only ranks 2016 as fifth lowest [with 4.5 (3.9) million km^2 according to the scatterometer (NSIDC) record].

3.2 Sea ice backscatter

The monitoring of sea ice backscatter may be used to discriminate Arctic FY and MY sea ice types, but it also can be applied to estimate sea ice motion by feature tracking (Zhao, Liu and Long, 2002; Lavergne et al., 2010), characterize Antarctic sea ice types (Morris, Jeffries and Li, 1998; Haas, 2001; Willmes, Haas and Nicolaus, 2011) or estimate the onset and duration of melt (Drinkwater and Liu, 2000; Howell et al., 2008). As already noted, the discrimination between Arctic FY and MY ice types using active microwaves is not without difficulty, its main hindrances being the seasonal variability of backscatter, including the effects of surface deformation, ice/snow metamorphism and a developing snow cover, or the appearance of summer signatures, more dependent on surface weather via processes such as wet snow attenuation and changes in brine temperature (Barber and Thomas, 1998). The annual cycles of MY ice coverage in the Arctic Ocean have been estimated using the QuikSCAT record (1999-2009) by (Kwok et al., 2009) using a fixed backscatter threshold from January to April,

Maria Belmonte Rivas 17/7/2018 17:57
Deleted: arrival

and by (Swan and Long, 2012) using a seasonally dependent backscatter threshold from November to April, to produce a multi-mission record extended forward in time onto 2014 using Ku-band Oceansat-2 scatterometer (OSCAT) data (Lindell and Long, 2016). In order to avoid the high-backscatter FY ice in the marginal ice zone (MIZ) from being classified as MY ice, (Kwok et al., 2009) introduced a static geographical mask, while (Lindell and Long, 2016) applied a MIZ correction algorithm based on the temporal persistence of the MY signature, along with a 40% sea ice concentration mask from passive microwave data.

For the determination of the time series of Arctic MY ice coverage, we adopt the single backscatter threshold approach. To avoid dealing with seasonal variability, we only use stable wintertime (March) backscatter maps, assuming that the backscatter signatures of the reference winter sea ice classes do not change with time. We also introduce a geographical mask to screen the high backscatter response from MIZ sea ice, which has been attributed to surface deformation by compression and irreversible snow/ice metamorphism after melt-freeze events (Voss et al., 2003) (Willmes et al., 2011). The geographical mask delimits the Arctic Basin (see red contours in Fig. 11) across the Fram Strait and Svalbard, to Severnaya Zemlya through Franz Josef Land (Kwok, Cunningham and Yueh, 1999). An additional line from Point Barrow to Wrangel Island also excludes the Chukchi Sea from the MY area estimations. The geographical mask omits the ubiquitous presence of multiyear ice in the Greenland Sea, or its episodic incursions into the marginal Chukchi, Barents and Kara Seas.

For the consistency of the record, the backscatter thresholds for MY ice detection at Ku and C-band are matched attending to their joint backscatter distributions and resulting spatial boundaries. The top panels in Figure 9 show the joint backscatter distributions of Arctic sea ice at C-band and Ku-band for the month of March in 2000 and 2008, before application of the geographical mask. Before masking, the joint distributions of wintertime sea ice backscatter are characterized by two elongated clusters: an upper cluster corresponding to perennial (MY) ice, and a lower one corresponding to seasonal (FY) ice (Ezraty and Cavanie, 1999). The cluster elongation gives account of geophysical variability, with perennial ice types getting brighter as they accumulate summer conditions, and seasonal ice types becoming brighter with surface deformation and/or metamorphism. Note that the range of backscatter variability associated to deformation and/or metamorphism in the lower seasonal ice cluster (~ 5 dBs) is comparable at C-band and Ku-band. The signature of volume scattering, though, is stronger at Ku-band, and effective at separating the rough FY and MY ice domains, which remain partly overlapping at C-band. The bottom panels in Figure 9 illustrate the effectiveness of the geographical mask at removing the MIZ signature, and how necessary this is for the definition of an effective separation threshold between FY and MY classes at C-band. Starting from the already established Ku-band threshold of -14.5 dB for the Quikscat VV backscatter, which would correspond to a MY sea ice fraction of 30% according to RADARSAT (Kwok, 2004), and aided by the correlation of the MY ice spatial boundaries at Ku and C-band (see Figure 11), an optimal threshold for MY detection using C-band VV backscatter (52.8 deg incidence) is found at -18.3 dB.

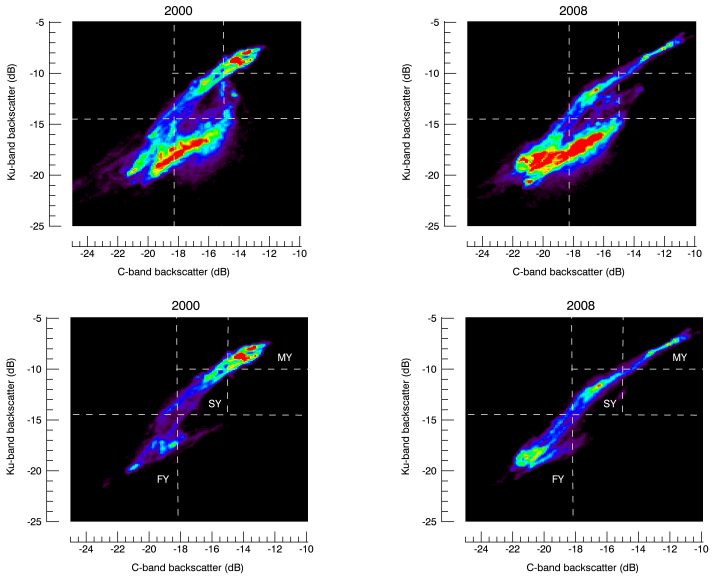

Figure 9: Joint distributions of wintertime (March) sea ice backscatter at C-band (x-axis) and Ku-band (y-axis), before (top row) and after (bottom row) applying the geographical mask in 2000 (left, ERS vs QSCAT) and 2008 (right, ASCAT vs QSCAT).

The left panels in Figure 10 show the marginal distributions of sea ice backscatter at Ku-band (top) and C-band (bottom) that correspond to the geographically masked joint distributions for the year 2000. The marginal backscatter distributions are characterized by two well-defined modes, associated to FY and MY sea ice types, connected by a transition range. Using spatially collocated Ku and C-band backscatter measurements, sea ice types in the transition range between the FY and MY modes may be further separated (see joint distribution in the bottom left panel of Fig. 9) into deformed FY (in the high range of the seasonal sea ice cluster), SY ice (in the low range of the perennial sea ice cluster), and FY-MY mixtures (along the path connecting the seasonal and perennial clusters). We note that an optimal threshold for MY detection should guarantee that most of the rough FY is removed from the MY category, while collecting various fractions of SY, MY, and FY-SY-MY mixtures.

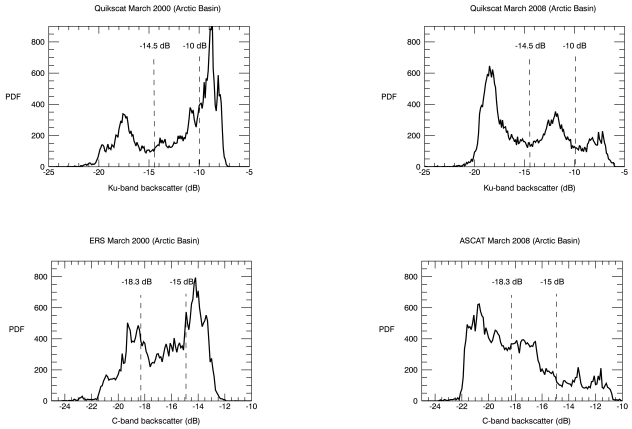

Figure 10: Marginal distributions of wintertime (March) sea ice backscatter collected at Ku-band (top row) and C-band (bottom row) after applying the geographical mask in 2000 (left column) and 2008 (right column).

After the anomalously large loss of Arctic sea ice that occurred in the summer of 2007, the shape of the wintertime sea ice backscatter histograms have become remarkable altered. The earlier bimodal (FY+MY) histograms have been replaced by trimodal distributions, featuring a smaller MY mode, and a new mode corresponding to SY ice emerging in the low range of the perennial sea ice cluster (see bottom right panel in Fig. 9). The emergence of the new SY mode is also evident in the marginal distribution of Ku-band backscatter for the year 2008 (see top right panel in Fig. 10), though more difficult to see in the marginal distribution of C-band data for the same year (see bottom right panel in Fig. 10, around -16.5 dB) because of the larger influence of deformed FY in this frequency and backscatter range. In order to monitor the evolution of the newly emerged SY mode, we split the perennial ice cluster into separate SY and old MY classes using an additional set of thresholds (-10 dB for Ku-band and -15 dB for C-band) whose location relative to the original FY and MY modes is shown in the joint and marginal distributions in Figs. 9 and 10.

The spatial distributions of the FY, SY and old MY classes that result from applying the single threshold approach on Ku and C-band backscatter images are displayed in Figure 11, along with the average sea ice age from the EASE-Grid dataset NSIDC-0611 from (Tschudi et al, 2016) for that period. The spatial distributions of the total MY ice class (defined as the sum of SY and old MY classes) from the scatterometer and the lagrangian sea ice age analyses are in general good agreement, although their depictions of the SY ice class differ somewhat. We note that the old MY sea ice class has a larger geographical spread in the lagrangian dataset, particularly over areas where MY ice is exposed to strong shear stress, such as in the Beaufort Sea. From the analysis of joint backscatter distributions, we know that the scatterometer SY class is bound to contain varying amounts of FY-SY-MY mixtures (and probably some deformed FY too), thus an inherent ambiguity remains

Maria Belmonte Rivas 17/7/2018 17:57
Deleted:). However

regarding the dominance of pure SY ice versus mixed FY-MY combinations in a cell labeled SY, particularly before 2007. On the other hand, the lagrangian dataset is monitoring the age of the oldest ice in a cell, regardless of its weight over other ice fractions, probably biasing this product towards a larger spread of old MY ice in the Arctic. Outside of the red contour that delineates the Arctic basin mask in the left and middle panels of Figure 11, we cannot register older ice reliably because of the strong backscatter from deformed MIZ ice.

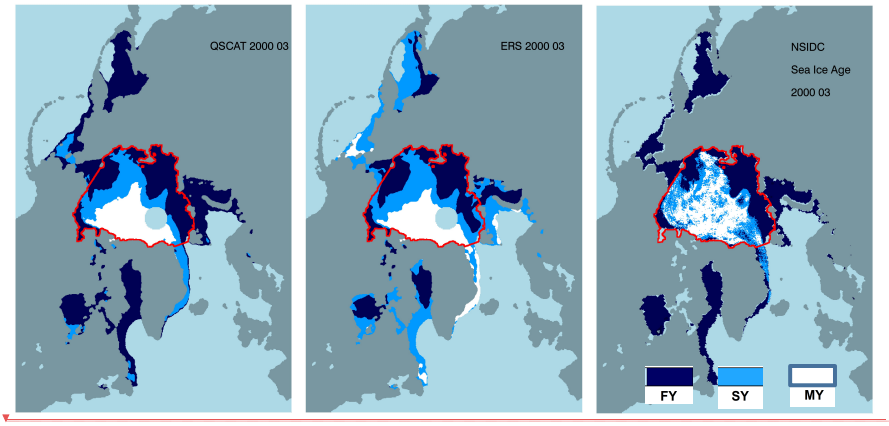

a) 2000

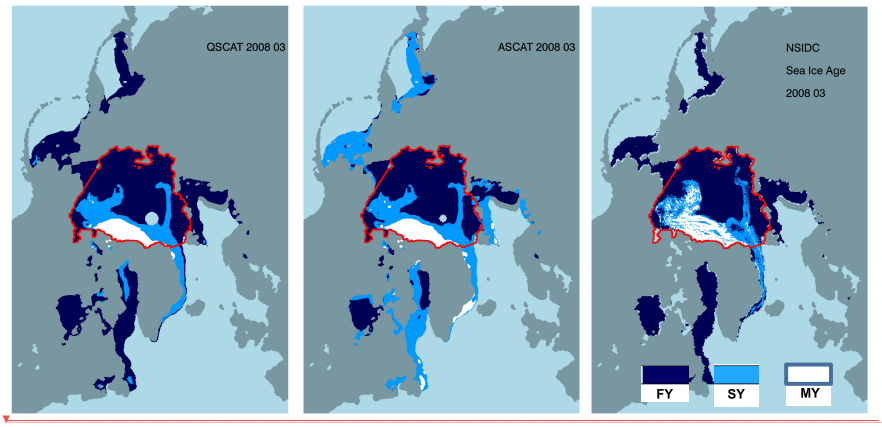

a) 2008

Figure 11: Geographical boundaries of wintertime FY (dark blue), SY (light blue) and MY (white) sea ice classes from Ku-band backscatter (left panel), C-band backscatter (middle panel) and NSIDC sea ice age (right panel) for 2000 (top row) and 2008 (bottom row). The contour of the geographical mask used to delimit the Arctic Basin is shown in red.

Maria Belmonte Rivas 17/7/2018 17:57

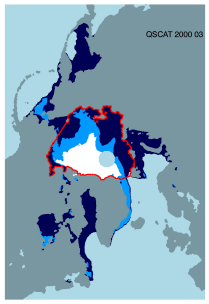

Deleted:

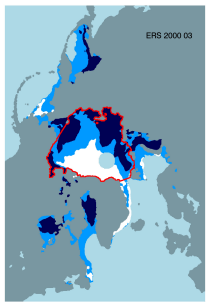

... [3]

Maria Belmonte Rivas 17/7/2018 17:57

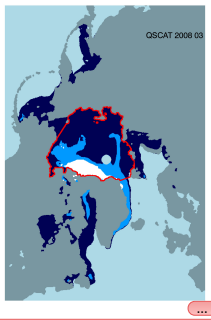

Deleted:

... [4]

The time series of the total MY sea ice extents, along with the extents of the separate SY and old MY class contributions calculated using the backscatter threshold approach on wintertime (March) data collected within the geographically masked Arctic Basin is shown in Fig. 12. All estimates exclude a common polar gap extent of 0.354 million km^2 around the North Pole. The evolution of the total MY sea ice extents derived from the scatterometer record agrees well with that derived from the NSIDC sea ice age dataset, showing a MY pack that begins to lose balance around 2005, after several consecutive years of decline, to finally collapse into a large loss in 2007. The partition into total SY and old MY ice extents is also similarly depicted in both datasets, regardless of discrepancies in their spatial distributions, providing further evidence to support our claim of a newly emergent SY ice mode. Figure 12 proves that the largest decline in Arctic MY ice is borne by loss of old MY ice after 2007, with a more steady production of SY ice partly buffering those losses, and driving later recovery events such as observed in 2014.

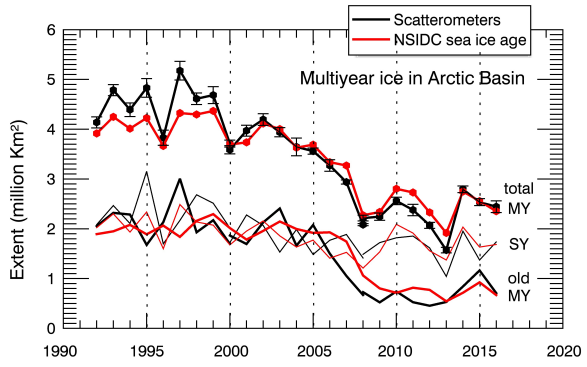

Figure 12: Time series of monthly wintertime (March) total multiyear sea ice extents (segmented into SY and older MY classes) within the Arctic Basin from the scatterometer (black) and the NSIDC sea ice age (red) records. Error bars are representative of the scatterometer class extent errors associated to a fixed backscatter threshold uncertainty of 0.1 dB (i.e. calibration accuracy).

Maria Belmonte Rivas 17/7/2018 17:57

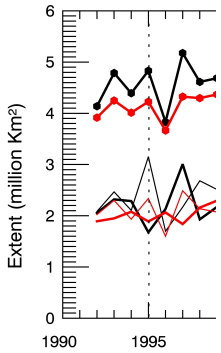

Deleted:

Thus far, we have justified the definition of a separate SY ice class after the emergence of a SY mode with an entity of its own in the scatterometer backscatter histograms. The differentiation of SY and lower concentration of MY using a single frequency remains an open question though. By construction, the scatterometer SY class will accommodate various fractions of deformed FY and FY-SY-MY mixtures in it, which we suggest may be differentiated from the homogenous SY ice signature by recourse to dual Ku-band and C-band observations. In this context, the reprocessed Ku-band Oceansat-2 record spanning the period from 2009 to 2014, also available in our scatterometer record, affords new opportunity to resolve this ambiguity. We note that the scatterometer record may be helpful as a check against currently developing algorithms for MY ice concentration based on satellite passive microwave or blended data, given that none of these latter products uses a separate tie point for SY ice, leaving the SY ice signature to be effectively interpreted as lower concentration MY ice. As an

illustration, Figure 13 shows the spatial distribution of MY ice according to a selection of state-of-the-art products for the month of March 2016, including sea ice age [from the scatterometer record, the NSIDC record of (Tschudi et al, 2016), and the SICCI record (Korosov et al, 2017)], MY ice concentration [from the OSISAF-403 (Aaboe et al, 2016), the U. Bremen algorithm (Ye et al, 2016), and the SICCI algorithm (Korosov et al, 2017)], and sea ice thickness from the AWI Cryosat-2 dataset (Ricker et al, 2014)]. The monthly averaged MY ice concentration is calculated directly over the daily MY ice concentrations from the SICCI and Bremen products. Note that the OSISAF-403 is not a sea ice concentration product but a FY/MY classification. In this case, a daily MY concentration is defined (100% for the MY class, 50% for the ambiguous class, and 0% for the FY and OW classes) and a monthly average MY concentration is calculated as above. The monthly averaged sea ice age is calculated over the weekly NSIDC grids (using weeks 9 to 12) and over the daily SICCI grids, and the SY ice class is defined for a monthly average sea ice age between 1.5 and 2.5 years.

Even though the general representation of MY ice is similar across all products, there are remarkable differences as well, mainly regarding the distribution of the old MY ice class north of the Canadian Arctic Archipelago (CAA, with large variations across the sea ice age records), and the presence of MY ice north of the Beaufort and Chukchi Seas (with notable differences between the MY ice concentration records). The ice thickness product is revealing in that the thickest sea ice (more than 3 m thick, and most likely associated to old MY ice) appears mostly confined to a thin strip along the CAA shore (see label A in Fig. 13g, in agreement with the scatterometer old MY ice class), and that it shows no traces of thick ice north of the Beaufort and Chukchi Seas (see label B in Fig. 13g, in disagreement with some of the MY concentrations, and the NSIDC sea ice age record). Further, we note a large extension of very thick ice north of Greenland (more than 3 m thick, see label C in Fig. 13g), which is labelled as SY ice in the scatterometer record (probably ridged SY ice converging into Fram Strait), which effectively appears as low concentration MY ice in the Univ. Bremen and SICCI algorithms, suggesting problems with the tie point definition in MY ice concentration algorithms (not in the OSISAF-403 dataset, because it is reports MY presence, not concentration). Finally, we find relative good agreement between the scatterometer SY ice class and the 2.0 m isoline from the ice thickness record, suggesting the utilization of the backscatter record as a reliable proxy for the estimation of thick sea ice thickness in the Arctic, much in the same way as (Tschudi, Stroeve and Stewart, 2016) propose relating the NSIDC sea ice age to ice thickness. Another interesting feature refers to the thin tongue of older ice extending across the Arctic Basin towards the New Siberian Islands (see label D in Fig. 13g), which is seen by all products, even faintly in the AWI sea ice thickness, but falls below the SY threshold in the scatterometer-based MY ice classification. We cannot offer an explanation for this feature at the moment, other than acknowledging that efforts towards ensuring the consistency among MY ice products in the Arctic should warrant further research.

Maria Belmonte Rivas 17/7/2018 17:57
Deleted:) north of Greenland,

Maria Belmonte Rivas 17/7/2018 17:57
Deleted: points

Maria Belmonte Rivas 17/7/2018 17:57
Deleted: taking into account its limitations (e.g. spurious high backscatter north of Franz-Josef Land).

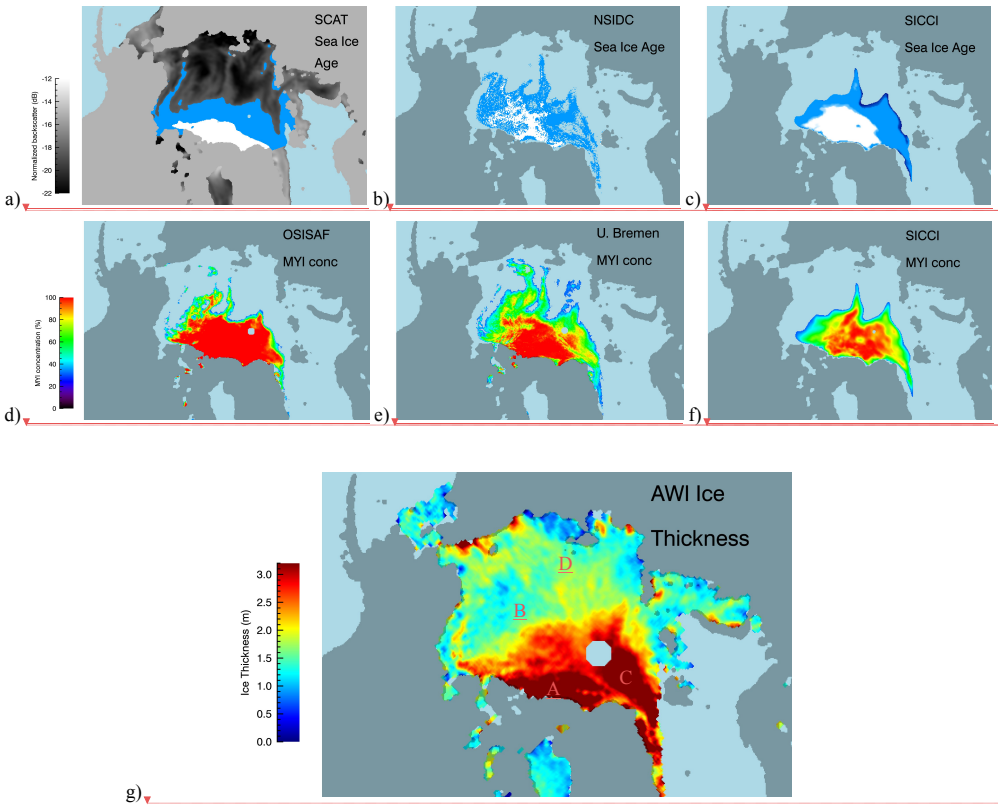

Figure 13: Different observation-based products for the representation of multiyear ice in March 2016: by sea ice age (top row, light blue is SY ice, white is old MY ice) from the scatterometer record (left), the NSIDC sea ice age (middle) and the SICCI algorithm (right); by multiyear ice concentration (middle row, MY>30%) from the OSISAF-403 (left), the Univ. Bremen algorithm (middle) and the SICCI algorithm (right); and by sea ice thickness (bottom plot). See text for labels.

Noting the lack of extensive in-situ validation sources for satellite-based datasets, one should rely on consistency among products as the best approach to check retrievals. Yet, the differences just noted in this section make it clear that further effort is necessary towards the optimal integration of active and passive microwaves, not only for the classification of sea ice types, but for the determination of summer sea ice edge and concentrations.

Maria Belmonte Rivas 17/7/2018 17:57
Deleted:

Maria Belmonte Rivas 17/7/2018 17:57
Deleted: ... [5]

Maria Belmonte Rivas 17/7/2018 17:57
Deleted: ... [6]

Maria Belmonte Rivas 17/7/2018 17:57
Deleted: ... [7]

Maria Belmonte Rivas 17/7/2018 17:57
Deleted: ... [8]

Maria Belmonte Rivas 17/7/2018 17:57
Deleted: ... [9]

Maria Belmonte Rivas 17/7/2018 17:57
Deleted: ... [10]

Maria Belmonte Rivas 17/7/2018 17:57
Formatted: current-selection

Maria Belmonte Rivas 17/7/2018 17:57
Deleted:

4 Conclusions

We present the first inter-calibrated long-term record of sea ice extents and backscatter derived from satellite scatterometer missions (ERS, QuikSCAT and ASCAT) extending from 1992 to present date. The scatterometer record, whose continuation into the future is guaranteed by the Metop ASCAT (B and C) and EPS-SG series, provides a valuable independent account of the state of Arctic and Antarctic sea ice cover, with daily sea ice extent and backscatter maps available at www.knmi.nl/scatterometer/ice_extents.

The scatterometer sea ice extents show excellent agreement with passive microwave fields in the fall and winter seasons, with differences within 0.25 million km^2 and an estimated ice edge accuracy of about 20 km, but show enhanced sensitivity to lower concentration and water-saturated sea ice conditions during the spring and summer months, as verified by numerous comparisons to MODIS and SAR imagery. The sea ice concentrations derived from satellite passive microwave brightness temperatures are affected by surface wetness during the melt season, typically underestimating the summer sea ice concentration and summer sea ice extent by up to 30%, and having a non-negligible impact on the ocean heat contents and surface fluxes when assimilated into reanalyses. In this context, the scatterometer sea ice extents and probabilities nicely complement the passive microwave products in providing a basis to monitor the occurrence of sea ice concentration errors due to surface wetness, and to delineate the expanse and evolution of the rotten late spring and summer ice classes.

The scatterometer backscatter maps also provide enhanced means to differentiate between sea ice types. Our study of the evolution of the wintertime seasonal (FY) and perennial (MY) ice classes in the Arctic Basin from 1992 to present day shows, in good agreement with the NSIDC sea ice age dataset, a MY ice pack that begins to lose balance around 2005, after several consecutive years of decline, to finally collapse into a record loss in 2007. The scatterometer maps also reveal the emergence of a new mode in the backscatter histograms after the record sea ice loss in 2007, bearing striking resemblance in both temporal evolution and spatial distribution with the SY ice class of the NSIDC sea ice age dataset. Monitoring the evolution of the complementary SY and old MY ice classes shows that the decline in the total MY ice extent observed in the Arctic has been driven by the loss of older MY ice, while a more steady production of SY ice has been acting to stabilize the losses, and contributed to later recovery events such as observed in 2014.

We note that the differentiation between SY, deformed FY and lower concentration (but older) MY ice may be difficult using single frequency backscatter. The simultaneous combination of C-band and Ku-band backscatter measurements allows further differentiation of sea ice types into deformed FY (high C-band, low Ku band), SY ice (low C-band, high Ku-band) and FY-MY mixtures (moderate Ku and C-band responses), suggesting new approaches to their disambiguation. As such, the combination of coincident Ku-band and C-band missions (such as during the Quikscat overlap in 2000 and 2008, or the Oceansat-2 overlap from 2009 to 2014), along with the use of contemporaneous multi-frequency passive microwave data,

Maria Belmonte Rivas 17/7/2018 17:57
Deleted: comparison to NIC sea ice charts.

Maria Belmonte Rivas 17/7/2018 17:57
Deleted: solid

Maria Belmonte Rivas 17/7/2018 17:57
Deleted: melt ponding

Maria Belmonte Rivas 17/7/2018 17:57
Deleted: the

Maria Belmonte Rivas 17/7/2018 17:57
Deleted: this newly emerged

Maria Belmonte Rivas 17/7/2018 17:57
Deleted: class reveals

Maria Belmonte Rivas 17/7/2018 17:57
Deleted: largest

Maria Belmonte Rivas 17/7/2018 17:57
Deleted: MYI ice is borne

Maria Belmonte Rivas 17/7/2018 17:57
Deleted: old

Maria Belmonte Rivas 17/7/2018 17:57
Deleted: with

Maria Belmonte Rivas 17/7/2018 17:57
Deleted: partly buffering those

Maria Belmonte Rivas 17/7/2018 17:57
Deleted: driving

Maria Belmonte Rivas 17/7/2018 17:57
Deleted:

Maria Belmonte Rivas 17/7/2018 17:57
Deleted: backscatter from

Maria Belmonte Rivas 17/7/2018 17:57
Deleted: . However, the

Maria Belmonte Rivas 17/7/2018 17:57
Deleted: a

Maria Belmonte Rivas 17/7/2018 17:57
Deleted: approach

Maria Belmonte Rivas 17/7/2018 17:57
Deleted: availability

Maria Belmonte Rivas 17/7/2018 17:57
Deleted:) affords new promise

affords renewed potential towards the generation of combined time-series of areal estimates of different ice classes, as demonstrated in (Remund, Long and Drinkwater, 2000), which can be used to guide reanalyses.

The scatterometer backscatter record is helpful as a check against currently developing algorithms for MY ice concentration based on satellite passive microwave or blended data, given that none of these latter products uses a separate tie point for SY ice, leaving the SY ice signature to be effectively interpreted as lower concentration MY ice. The comparison of a selection of state-of-the-art datasets for the representation of MY ice (including sea ice age, MY ice concentration and ice thickness estimates) in the Arctic reveals some notable inconsistencies, mainly regarding the ambiguity between compact SY and lower MY ice fractions, the spatial distribution of old MY ice in the sea ice age records, and the apparently spurious presence of MY ice in the Central Arctic in some of the MY concentration records derived from satellite passive microwaves. The relative good agreement between the backscatter-based sea ice (FY, SY and older MY) classes and the ice thickness record from Cryosat suggests its applicability as a reliable proxy in the historical reconstruction of sea ice thickness in the Arctic.

Noting the lack of extensive in-situ validation sources for satellite-based datasets, one should rely on consistency among products as the best approach to check retrievals. Yet, the differences among state-of-the-art products noted in this paper make it clear that further effort is necessary towards the optimal integration of active and passive microwaves, not only for the classification of sea ice types, but for the determination of summer sea ice edge and concentrations.

Acknowledgments

The authors would like to acknowledge the financial support of the ESA Scirocco project, the EUMETSAT OSI-SAF for the provision of backscatter data, our KNMI colleague Jeroen Verspeek for his insights, and the NASA and NSIDC public data archives as essential towards the completion of this activity. Processing of the AWI CryoSat-2 (PARAMETER) ice thickness is funded by the German Ministry of Economics Affairs and Energy (grant: 50EE1008) and data obtained from http://www.meereisportal.de (grant: REKLIM-2013-04).

References

Aaboe, S., Breivik, L. A. and Eastwood, S.: ATBD for the OSI SAF Global Sea Ice Edge and Type Product, OSI SAF report CDOP2/MET-Norway/SCI/MA/208, http://osisaf.met.no/docs/osisaf_cdop2_ss2_atbd_sea-ice-edge_type_v1p2.pdf, 2015.

Aaboe, S., Breivik, L. A., Eastwood, S. and Sorensen, A.: Global Sea Ice Edge and Type Validation Report, OSI SAF report CDOP2/MET-Norway/SCI/RP/224, http://osisaf.met.no/docs/osisaf_cdop2_ss2_valrep_sea-ice-edge-type_v2p1.pdf, 2016.

Barber, D. G. and Thomas, A.: The influence of cloud cover on the radiation budget, physical properties and microwave scatterin coefficients of first-year and multi-year ice, IEEE T. Geosci. Remote Sens., 36(1), 38-50, 1998.

Belmonte Rivas, M., Stoffelen, A., "Near Real-Time sea ice discrimination using SeaWinds on QuikSCAT", OSI SAF Visiting Scientist Report, SAF/OSI/CDOP/KNMI/TEC/TN/168, https://cdn.knmi.nl/system/data_center_publications/files/000/068/084/original/sea_ice_osi_saf_final_report.pdf?1495621021, 2009.

Belmonte Rivas, M. and Stoffelen, A.: New Bayesian algorithm for sea ice detection with QuikSCAT, IEEE T. Geosci. Remote Sens., 49(6), 1894-1901, 2011.

Belmonte Rivas, M., Verspeek, J., Verhoef, A. and Stoffelen, A.: Bayesian sea ice detection with the Advanced Scatterometer ASCAT, IEEE T. Geosci. Remote Sens., 50(7), 2649-2657, 2012.

Belmonte Rivas, M., Stoffelen, A., Verspeek, J., Verhoef, A., Neyt, X. and Anderson, C.: Cone metrics: a new tool for the intercomparison of scatterometer records, IEEE J. Sel. Topics Appl. Earth Observ. In Remote Sens., 10(5), 2195-2204, 2017.

Cavalieri, D. J., Parkinson, C. L., Gloersen, P. and Zwally, H.: Sea ice concentrations from NIMBUS-7 SMMR and DMSP SSM/I-SSMIS passive microwave data (version 1), Boulder, CO, USA, NASA National Snow and Ice Data Center Distributed Active Archive Center. Digital media, 2015. [Note: from 1992 through 2015, the reprocessed data labelled NSIDC-0051 are used; to complete the series in 2016, the NRT data labelled NSIDC-0081 are used].

Comiso, J.C., Kwok, R.: Surface and radiative characteristics of the summer Arctic sea ice cover from multisensor satellite observations, J. Geophys. Res., 101(C12), pp 28397-28416, 1996.

Drinkwater, M. R. and Liu, X.: Seasonal to Interannual variability in Antarctic sea ice surface melt, IEEE T. Geosci. Remote Sens., 38(4), 1827-1842, 2000.

Eisenman, I., Meier, W. N. and Norris, J.R.: A spurious jump in the satellite record: has Antarctic sea ice expansion been overestimated?, The Cryosphere, 8, 1289-1296, 2014.

Haas, C.: The seasonal cycle of ERS scatterometer signatures over perennial Antarctic sea ice and associated surface ice properties and processes, Annals Glaciology, 33(1), pp 69-73, 2001.

Hill, J. C. and Long, D. G.: Extension of the QuikSCAT sea ice extent data set with OSCAT data, IEEE Geosci. Remote Sens. Lett., 14, 92-96, 2017.

Hirahara, S., Alonso Balmaseda, M., Boisseson, E., Hersbach, H.: Sea surface temperature and sea ice concentration for ERA5, ERA report series, 26, ECMWF, 2016.

Howell, S., Tivy, A., Yackel, J. J., Else, B. and Duguay, C. R.: Changing sea ice parameters in the Canadian Arctic Archipelago: Implications for the future presence of multiyear ice, J. Geophys. Res., 113(C09030), 2008.

Ivanova, N., Pedersen, L.T., Tonboe, R.T., Kern, S., Heygster, G., Lavergne, T., Sorensen, A., Saldo, R., Dybkjaer, G., Brucker, L., Shokr, M.: Inter-comparison and evaluation of sea ice algorithms: towards further identification of challenges and optimal approach using passive microwave observations, The Cryosphere, 9, 1797-1817, 2015.

Kern, S., Rösel, A., Pedersen, L. T., Ivanova, N., Saldo, R., and Tonboe, R. T.: The impact of melt ponds on summertime microwave brightness temperatures and sea-ice concentrations, The Cryosphere, 10, 2217-2239, 2016.

Korosov, A.A., Rampal, P., Perdersen, L.T., Saldo, R., Ye, Y., Heygster, G., Lavergne, T., Aaboe, S., Girard-Ardhuin, F., A new tracking algorithm for sea ice age distribution estimation, The Cryosphere Discussions, https://doi.org/10.5194/tc-2017-250, 2017.

Kwok, R., Comiso, J. C., Cunningham, G. F.: Seasonal characteristics of the perennial ice cover of the Beaufort Sea, J. Geophys. Res., 101(C12), 28417-28439, 1996.

Kwok, R., Cunningham, G. F., and Yueh, S.: Area balance of the Arctic Ocean perennial ice zone: October 1996 to April 1997, J. Geophys. Res., 104(C11), pp 25747-25759, 1999.

Kwok, R.: Annual cycles of multiyear sea ice coverage of the Arctic Ocean: 1999-2003, J. Geophys. Res., 109(C11004), doi:10.1029/2003JC002238, 2004.

Kwok, R., Cunningham, G. F., Wensnahan, M., Rigor, I., Zwally, H. J. and Yi, D.: Thinning and volume loss of the Arctic Ocean sea ice cover: 2003-2008, J. Geophys. Res., 114(C07005), doi:10.1029/2009JC005312, 2009.

Lavergne, T., Eastwood, S., Tehhah, Z., Schyberg, H. and Breivik, L. A.: Sea ice motion from low-resolution satellite sensors: an alternative method and its validation in the Arctic, J. Geophys. Res., 115(C10032), 2010.

Lindell, D. B. and Long, D. G.: Multiyear Arctic sea ice classification using OSCAT and QuikSCAT, IEEE T. Geosci. Remote Sens., 54, 167-175, 2016.

Meier, W., N. and Stroeve, J.: Comparison of sea-ice extent and ice edge location estimates from passive microwave and enhanced resolution scatterometer data, Ann. Glaciol., 40, 65-70, 2008.

Meier, W. N., Fetterer, F., Stewart, J. S. and Helfrich, S.: How do sea-ice concentrations from operational data compare with passive microwave estimates? Implications for improved model evaluations and forecasting, Ann. Glaciol., 56(69), 332-340, doi: 10.3189/2015AoG69A694, 2015.

Morris, K., Jeffries, M. O. and Li, S.: Sea ice characteristics and seasonal variability of ERS-1 SAR backscatter in the Bellingshausen Sea, Antarctic Sea Ice: Physical Processes, Interactions and Variability, Antarctic Research Series, 74, pp 213-242, 1998.

NSIDC: 2016 ties with 2007 for second lowest Arctic sea ice minimum, http://nsidc.org/arcticseaicenews/2016/09/2016-ties-with-2007-for-second-lowest-arctic-sea-ice-minimum, September 15th, 2016.

Otosaka, I., Belmonte Rivas, M. and Stoffelen, A.: Bayesian sea ice detection with the ERS Scatterometer ESCAT, submitted to IEEE T. Geosci. Remote Sens., 2017.

Remund, Q.P., Long, D.G. and Drinkwater, M.R.: An iterative approach to multisensory sea ice classification, IEEE T. Geosci. Remote Sens, 38(4), 1843-1856, 2000.

Remund, Q. P. and Long, D. G.: A decade of QuikSCAT scatterometer sea ice extent data, IEEE T. Geosci. Remote Sens, 52(7), 4281-4290, 2014.

Ricker, R., Hendricks, S., Helm, V., Skourup, H. and Davidson, M., Sensitivity of CryoSat-2 Arctic sea-ice freeboard and thickness on radar-waveform interpretation, The Cryosphere, 8 (4), 1607-1622, doi:10.5194/tc-8-1607-2014, 2014.

Stoffelen, A., Verspeek, J., Vogelzang, J. and Verhoef, A.: The CMOD7 Geophysical Model Function for ASCAT and ERS wind retrievals, IEEE J. Sel. Topics Appl. Earth Observ. In Remote Sens., 10(5), pp. 2123-2134, 2017.

Maria Belmonte Rivas 17/7/2018 17:57
Formatted: Font:Times New Roman

Swan, A. M. and Long, D. G.: Multiyear Arctic sea ice classification using QuikSCAT, IEEE T. Geosci. Remote Sens, 50(9), 3317-3326, 2012.

Thomas, D. R.: Arctic sea ice signatures for passive microwave algorithms, J. Geophys. Res., 98(C6), 10037-10052, doi:10.1029/93JC00140, 1993.

Titchner, H.A., Rayner, N.A.: The Met Office Hadley Center sea ice and sea surface temperature data set, version 2: 1. Sea ice concentrations, J. Geophys. Res. Atmos., 119, 2864-2889, doi:10.1002/2013JD020316, 2014.

Tonboe, R.T., Eastwood, S., Lavergne, T., Sorensen, A.M., Rathman, N., Dybkjaer, G., Pedersen, L.T., Hoyer, J., Kern, S., The EUMETSAT sea ice concentration climate data record, The Cryosphere, 10, 2275-2290, 2016.

Tschudi, M.A., Fowler, C, Maslanik, J.A., and Stroeve, J.: Tracking the movement and changing surface characteristics of Arctic sea ice. IEEE J. Selected Topics in Earth Obs. And Rem. Sens., 10.1109/JSTARS.2010.2048305, 2010.

Tschudi, M.A., Stroeve, J. and Stewart, J.S.: Relating the age of Arctic sea ice to its thickness, as measured during NASA's ICEsat and IceBridge, *Remote Sens.* **2016**, *8*(6), 457, doi:10.3390/rs8060457, 2016.

Tschudi, M., Fowler, C., Maslanik, J, Stewart, J. S., and Meier, W.: EASE-Grid Sea Ice Age (V3). Boulder, Colorado USA: NASA National Snow and Ice Data Center Distributed Active Archive Center, 2016.

Ulaby, F.T., Moore, R.K., and Fung, A.K.: Microwave Remote Sensing: Active and Passive, Volume III: From Theory To Applications, Artech House Publishers, London, UK, 1981.

Verhoef, A. and Stoffelen, A.: Reprocessed SeaWinds L2 winds Product User Manual (PUM), Version 1.4, SAF/OSI/CDOP2/KNMI/TEC/MA/220, EUMETSAT, February 2016.

Verhoef, A. and Stoffelen, A.: Algorithm Theoretical Basis Document (ATBD) for the OSI SAF wind products, Version 1.4, SAF/OSI/CDOP2/KNMI/SCI/MA/197, EUMETSAT, February 2017.

Voss, S., Heygster, G., Ezraty, R., Improving sea ice type discrimination by the simultaneous use of SSM/I and scatterometer data, Polar Research, 22(1), 35-42, 2003.

Maria Belmonte Rivas 17/7/2018 17:57
Deleted:

Maria Belmonte Rivas 17/7/2018 17:57
Formatted: Font:+Theme Body, Font color: Auto

Maria Belmonte Rivas 17/7/2018 17:57
Formatted: Font:+Theme Body

Maria Belmonte Rivas 17/7/2018 17:57
Formatted: Font:+Theme Body

Willmes, S., Haas, C. and Nicolaus, M.: High radar backscatter regions on Antarctic sea ice and their relation to sea ice and snow properties and meteorological conditions, International Journal of Remote Sensing, 32(14), pp 3967-3984, 2011.

Ye, Y., Shokr, M., Heygster, G., Spreen, G., Improving multiyear ice concentration estimates with ice drift, Remote Sens., 8(5), 397, doi:10.3390/rs8050397, 2016.

Zhao, Y., Liu, A. K. and Long, D. G.: Validation of sea ice motion from QuikSCAT with those from SSM/I and buoy, IEEE T. Geosci. Remote Sens, 40(6), 1241-1246, 2012.